THE UNIVERSITY OF ALBERTA

PARAMETRIC ANALYSIS ON THE SLIM-TUBE DISPLACEMENT TESTS.

by

© AKLI NOUAR

A THESIS

SUBMITTED TO THE FACULTY OF GRADUATE STUDIES AND RESEARCH

IN PARTIAL FULFILMENT OF THE REQUIREMENTS FOR THE DEGREE

OF MASTER OF SCIENCE

IN

PETROLEUM ENGINNERING

DEPARTMENT OF MINERAL ENGINNERING

EDMONTON, ALBERTA

Spring, 1984

THE UNIVERSITY OF ALBERTA

RELEASE FORM

NAME OF AUTHOR Akli NOUAR

TITLE OF THESIS PARAMETRIC ANALYSIS ON THE SLIM-TUBE DISPLACEMENT TESTS

DEGREE FOR WHICH THESIS WAS PRESENTED MASTER OF SCIENCE

YEAR THIS DEGREE GRANTED Spring, 1984

Permission is hereby granted to THE UNIVERSITY OF ALBERTA LIBRARY to reproduce single copies of this thesis and to lend or sell such copies for private, scholarly or scientific research purposes only.

The author reserves other publication rights, and neither the thesis nor extensive extracts from it may be printed or otherwise reproduced without the author's written permission.

(SIGNED) A. N. Nouar

PERMANENT ADDRESS:
26 Rue Parmentier
Birmandreis Alger
ALGERIE (ALGERIA)

DATED December 2nd, 1983

THE UNIVERSITY OF ALBERTA

FACULTY OF GRADUATE STUDIES AND RESEARCH

The undersigned certify that they have read, and recommend to the Faculty of Graduate Studies and Research, for acceptance, a thesis entitled PARAMETRIC ANALYSIS ON THE SLIM-TUBE DISPLACEMENT TESTS submitted by Akli NOUAR in partial fulfilment of the requirements for the degree of MASTER OF SCIENCE in PETROLEUM ENGINNERING.

.....

Supervisor

.....

.....

Date December 8nd, 1983

ABSTRACT

The reservoir pressure required for the development of a dynamic vapourizing gas miscible drive is often determined experimentally by what is referred to as the "slim-tube" displacement test.

Early work has shown that, provided the displacement is stable, the determination of the minimum miscibility pressure is only a function of the thermodynamic conditions (nature of fluids and temperature).

The purpose of this investigation was to verify whether the above conclusion can be drawn for conventional tests carried out in flat slim-tube coils. This has been done by examining the effect of tube length and injection rate on the displacement efficiency at various pressures covering the immiscible and multiple-contact miscible displacements.

It was found that the interplay of gravity forces and viscous forces has an effect on the results, and in the early stage of the displacement supercritical flow occurs for the injection rates studied. These rates are of the same order of magnitude as those considered by other experimenters. Increasing the length of the model, on the other hand, tends to have an overall stabilizing effect on the results. For short cores, the usual indicators cannot be trusted to establish the minimum miscibility pressure. The use of longer cores yields the best estimate of the minimum miscibility pressure.

AKNOWLEDGEMENTS

The author is especially grateful to Dr. D.L. Flock for his guidance in this study.

Aknowledgement is made to Dr. R.G. Bentsen for his helpful advices.

Thanks are due to the ALBERTA OIL SANDS TECHNOLOGY AND RESEARCH AUTHORITY and the PETROLEUM AID TO EDUCATION for partial financial support.

Thanks are also due to Messrs. J. Gibeau, B. Smith and J. szuroski who helped in the set up of the experimental apparatus.

Table of Contents

Chapter		Page
1.	INTRODUCTION	1
2.	Mechanism of High Pressure Gas Displacement The Vapourizing Gas Drive	4
	2.1 Introduction.	4
	2.2 Phase Behaviour Representation of a Multicomponent HC-System.	5
	2.3 Basic Displacement Mechanisms of a Vapourizing Gas Drive.	8
	2.3.1 Immiscible Case.	9
	2.3.2 Multiple-contact Miscible Case (or Dynamic Miscibility).	14
	2.3.3 First-contact Miscible Case.	19
	2.4 Definition of the Minimum Miscibility Pressure.	20
3.	Methods for Estimating the MMP for a Vapourizing Gas Drive	23
	3.1 Introduction.	23
	3.2 Pseudo-ternary Diagram Method.	24
	3.3 PVT-cell Determination of the MMP.	28
	3.3.1 The Immiscible Case.	29
	3.3.2 The Multiple-contact Miscible Case.	31
	3.4 Slim-tube Test Method.	33
4.	Stability Considerations in Slim-Tube Displacements	37
	4.1 Introduction.	37
	4.2 Stability Considerations for a Vapourizing Gas Drive.	39
	4.3 Onset of Instability During Two-phase Immiscible Displacement.	45
	4.4 Stability Considerations of Miscible Displacements.	48

4.5 Applications to Vapourizing Gas Displacements Conducted in Horizontal Slim-tubes. 53

5. Experimental Apparatus and Experimental Procedure ...56

5.1 Description of the Slim-tube Apparatus. 56

5.2 Experimental Procedure. 59

6. Results and Discussion 65

6.1 Line of Investigation. 65

6.2 Discussion of Results. 66

6.2.1 Effect of Length and Injection Rate on Recovery. 66

6.2.1.1 Effect of Length. 66

6.2.1.2 Effect of Injection rate. 71

6.2.2 Effect of Length and Injection Rate on Concentration Profile. 73

6.2.2.1 Effect of Length. 73

6.2.2.2 Effect of Injection Rate. 79

6.2.3 Analysis of the Extreme Cases. 80

7. CONCLUSIONS 84

7.1 RECOMMENDATIONS 85

NOMENCLATURE 87

REFERENCES 89

APPENDIX 1: Definition of Dispersion Coefficient in Porous Media 92

APPENDIX 2: Effect of Molecular Diffusion and Convective Mixing in Multicomponent Systems 99

SAMPLE PROBLEM: First-contact Miscible Displacement of Methane-decane by Methane-butane 106

List of Figures

Figure 1 - Phase behaviour of a hc-system at constant pressure and temperature 6

Figure 2-A - Phase diagram; immiscible case; starting stage (P1,T) 10

Figure 2-B - Saturation profile 10

Figure 3-A - Phase diagram; immiscible case; final stage (P1,T) 12

Figure 3-B - Saturation profile 12

Figure 4-A - Phase diagram; dynamic miscibility; starting stage (P2,T) 15

Figure 4-B - Saturation profile 15

Figure 5-A - Phase diagram; dynamic miscibility; final stage (P2,T) 16

Figure 5-B - Saturation profile 16

Figure 6-A - Idealized representation of porous media 18

Figure 6-B - Representation of the effect of convective mixing on a phase diagram 18

Figure 7-A - Phase diagram; first-contact miscible case (P3,T) 21

Figure 7-B - Saturation profile 21

Figure 8 - Phase behaviour of a 4-component system at constant pressure and temperature 27

Figure 9 - Representation of a PVT-cell multiple batch-contact on a ternary diagram (immiscible case) .30

Figure 10 - Representation of a PVT-cell multiple batch-contact on a ternary diagram (multiple-contact miscible case) 32

Figure 11 - Relative positions of fluid 1 and fluid 2 as related to the conventions adopted in the statement of Equations (6) and (8) 42

Figure 12 - Flow regimes in a two-dimensional, uniform linear system 49

Figure 13 - Slim-tube apparatus schematic 57

Figure 14 - Phase behaviour of n-butane - n-decane system, T=23C 63

Figure 15 - Methane - n-butane - n-decane coexisting phases, T=71C 67

Figure 16 - Effect of tube length and injection rate on recovery at 1.2 PVinj for various operating pressures 69

Figure 17 - Correlation of MMP vs mole % butane in butane-decane mixture (T=71C) 74

Figure 18 - Effect of tube length and injection rate on concentration profile (miscible case), V = 20.7 m/d ..75

Figure 19 - Effect of tube length and injection rate on concentration profile (miscible case), V = 41.5 m/d ..75

Figure 20 - Effect of tube length and injection rate on concentration profile (miscible case), V = 84.8 m/d ..75

Figure 21 - Effect of tube length and injection rate on concentration profile (near-miscible case), V = 20.7 m/d 76

Figure 22 - Effect of tube length and injection rate on concentration profile (near-miscible case), V = 41.5 m/d 76

Figure 23 - Effect of tube length and injection rate on concentration profile (near-miscible case), V = 84.8 m/d 76

Figure 24 - Effect of tube length and injection rate on concentration profile (immiscible case), V = 20.7 m/d 78

Figure 25 - Effect of tube length and injection rate on concentration profile (immiscible case), V = 41.5 m/d 78

Figure 26 - Effect of tube length and injection rate on concentration profile (immiscible case), V = 84.8 m/d 78

Figure 27 - Effect of tube length and injection rate on recovery vs pressure for the extreme cases 81

Figure 28 - Effect of tube length and injection rate on concentration profile for the extreme cases, P = 24,118. Kpa 82

Figure 29 - Effect of tube length and injection rate on concentration profile for the extreme cases, P = 20,673. Kpa 82

Figure 30 - Effect of tube length and injection rate on concentration profile for the extreme cases, P = 17,228. Kpa 82

Figure 31 - Equivalent system of an ideal porous medium saturated with water of resistivity Rw 95

Figure 32 - Comparison of composition path on the phase diagram 115

List of Tables

Table 1 - Experimental procedures and criteria for MMP determination 35

Table 2 - Slim-tube physical characteristics 58

Table 3 - Summary of operating variables 68

Table 4 - Concentration distribution with respect to length; solution to the exact solution approximated by the ERFC function 113

1. INTRODUCTION

For many decades, petroleum engineers have been working to improve on the oil recovery techniques. They have focussed on maximizing the recovery of oil from underground reservoirs in the most economical way. In practice, only a small fraction of the oil in place is recovered by conventional production schemes, such as primary depletion. Secondary schemes, pressure maintenance and water flooding, increase the overall recovery. However, the oil is not totally recovered due, to some extent, to the interfacial tension existing between the phases present in the porous medium.

Tertiary recovery methods were subsequently developed in order to alleviate the problem of low secondary recovery. The idea was to eliminate or at least reduce the effect of the interfacial phenomena. The obvious approach would be to use a displacing fluid which is completely miscible with the reservoir oil, for instance a solvent. However, the choice of fluids miscible with crude oil is severly limited in practice by economic considerations. Different viable operations have been proposed; they are briefly outlined below.

Displacement by a slug of rich gas followed by dry gas: In this type of displacement, a predertermined volume of liquified petroleum gas (mainly propane and butane) is first injected, which in turn is driven by an inexpensive lean gas. The slug acts as a buffer zone, mutually miscible with

the displacing and displaced fluids.

Vapourizing gas drive: In this case, the mechanism consists of an enrichment of the lean displacing gas (stripping of the intermediate hydrocarbons present in the oil) until miscibility is dynamically initiated. Conditions favourable to this type of displacement are usually encountered in reservoirs with rather volatile light oils and at high pressures.

Condensing gas drive: This type of displacement is similar to the previous case, in the sense that miscibility is dynamically initiated through multiple contacts between the concurrently flowing phases. However, the enrichment process is reversed, and consists of a condensation of the intermediate hydrocarbons present in the wet gas, upon contact with the reservoir oil. Conditions favourable to this type of displacement are found in reservoirs with medium API gravity oil and moderate pressures.

The following discussion and experimental results will deal with the vapourizing gas drive case, where the displacing fluid is a lean gas. When planning to exploit a reservoir by the above process, one should first determine the conditions necessary to achieve miscibility. The composition of the oil and the temperature of the reservoir being fixed, one needs to find the minimum operating pressure which must be maintained to ensure miscibility.

The minimum miscibility pressure is often determined experimentally by what is referred to as the slim-tube

displacement test. However, as pointed out by Orr *et al.*(1), there is no general consensus as to the experimental procedures or the criteria defining the minimum miscibility pressure. They observed that displacement lengths ranged from 1.5 to 25.6m, flow geometries varied from vertical to flat coils to spirals, and flow velocities varied over nearly two orders of magnitude. The minimum miscibility pressure is generally determined from criteria based on recovery at some pore volume injected and/or, on the visual observation of the transition zone in a sight glass at the outlet of the model. These criteria will be discussed in more detail in a later section.

The primary objective of this research project was to carry out a parametric analysis of the slim-tube displacement test. The experiments were conducted on a flat slim-tube coil apparatus, as it is the most commonly used in the industry. The effect of tube length and injection rate on displacement efficiency, namely recovery and shape of the effluent gas concentration profile, and consequently their effects on the criteria used for estimating the minimum miscibility pressure were examined.

2. Mechanism of High Pressure Gas Displacement
The Vapourizing Gas Drive

2.1 Introduction.

High pressure gas displacement is a process by which oil is displaced by a gas at high pressure and is characterized by a mass transfer between the two phases which, initially, are not in thermodynamic equilibrium. Depending on the compositions of the gaseous phase injected and the oil displaced, and the average operating conditions of pressure and temperature, three types of displacements may occur, namely:

a) immiscible displacement

b) multiple-contact or dynamic miscible displacement

c) first-contact miscible displacement.

We will restrict the discussion to the case of a vapourizing gas drive, a special case of high pressure gas drive. In these conditions, the injected gas would be poor in intermediate components, C2-C6, while the oil would be rich in these components. The mass transfer between the concurrently flowing phases would consist essentially of stripping these intermediates by the gas phase, as well as the solution of the light ends, C1-N2, in the oil, until thermodynamic equilibrium is established.

A thorough understanding of the displacement mechanism is necessary, in order to introduce the concept of minimum miscibility pressure. From such an analysis, it is also

possible to describe the basis for the criteria defining it.

2.2 Phase Behaviour Representation of a Multicomponent HC-System.

In general, a high pressure gas displacement is characterized by a mass transfer between the concurrently flowing phases. Thermodynamic considerations should therefore be accounted for, such as the phase behaviour of the hydrocarbon system of interest. The composition of a complex hydrocarbon system can be divided into three pseudo-groups, namely:

the light ends, C1-N2
the intermediates, C2-C6
and the heavy ends, C7+.

At some fixed pressure and temperature, the phase behaviour of a multicomponent hc-system can conveniently be represented on a ternary diagram, by means of these pseudo-groups. However, we must keep in mind that such a representation is not rigorous in a thermodynamic sense.

Figure 1 is such a representation. The ternary diagram is a compositional diagram. Each apex of the triangle corresponds to a pure pseudo-group or to 100 mole% of the component Cx, where:

C1: refers to the light-ends pseudo-group
C2: refers to the intermediates pseudo-group
C3: refers to the heavy-ends pseudo-group.

Let us suppose that Ng moles of a fluid from region (A) come

FIG 1

PHASE BEHAVIOUR OF A HC-SYSTEM

AT CONSTANT PRESSURE AND TEMPERATURE

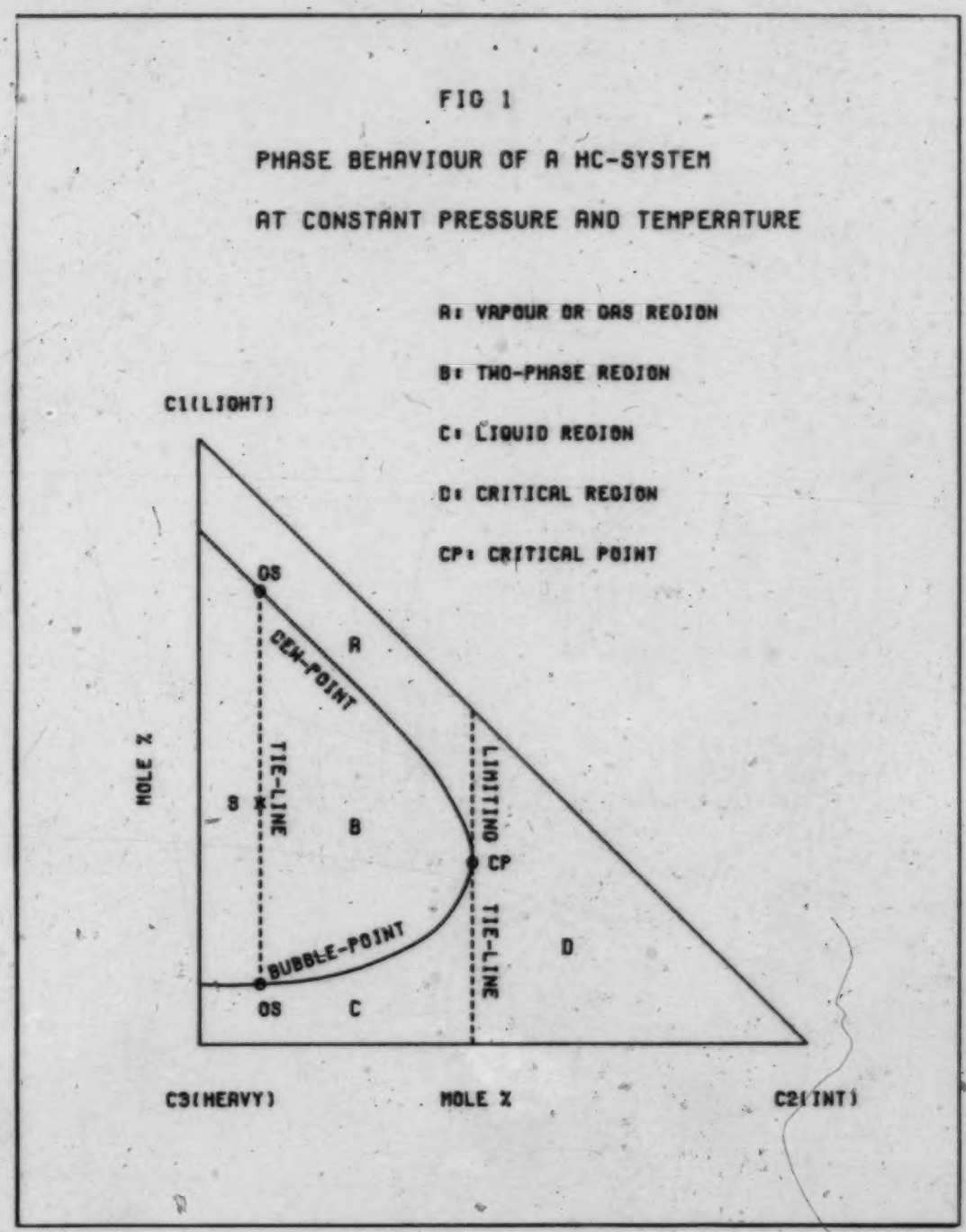

into contact with N1 moles of a fluid from region (C), and that equilibrium between the two phases is established. The resulting system, depending on its overall composition, will be located in either the region (C), (liquid phase), the region (B) (two-phase region), or the region (A) (the gas phase). As more gas from region (A) is brought into the system, there will be a transition in the phase behaviour of such a system from an initial liquid state, to a coexistence of a gaseous and liquid phases, and eventually to a single gaseous phase. The two-phase region is bounded by the phase envelope which comprises:

the dew-point curve:

loci of points where the gas phase is in equilibrium with an infinitesimal amount of liquid.

the bubble-point curve:

loci of points where the liquid phase is in equilibrium with an infinitesimal amount of gas.

The two curves meet at the critical point, (CP), where all the properties of the coexisting liquid and gaseous phases become identical.

If a hydrocarbon system has a composition that places it inside the phase envelope, two phases will result at equilibrium. The point representing the composition of the gas phase will be located on the dew-point curve, and the point representing the liquid phase composition, on the bubble-point curve. The line connecting these points is

referred to as a tie-line. Each point, (S), of this tie-line represents the overall composition of a hc-system which, at equilibrium, will have gas and liquid phases of compositions corresponding to the intersection of the tie-line with the dew-point and bubble-point curves, respectively (GS,OS). The relative amounts of gas and liquid are given by the lever rule:

$$\frac{NGS}{NOS} = \frac{\overline{SOS}}{\overline{SGS}} \quad \text{and} \quad NS = NGS + NOS \qquad (1)$$

where,

NGS = number of moles in gas phase

NOS = number of moles in liquid phase

NS = total number of moles of the system

$\overline{SGS}$ = distance between points (S) and (GS)

$\overline{SOS}$ = distance between points (S) and (LS)

In region (D), we cannot distinguish a gaseous phase from a liquid phase. This region is bounded by the limiting tie-line, which is defined as the line tangent to the phase envelope at the critical point.

2.3 Basic Displacement Mechanisms of a Vapourizing Gas Drive.

A vapourizing gas drive is a special case of a high pressure gas displacement. The displacing phase is a lean gas poor in intermediates, while the displaced phase is an oil, rich in these components. In general, at reservoir

conditions, the temperature and the displacing and displaced fluid compositions are fixed. The only variable which can be altered is the displacement pressure. Depending on the prevailing pressure, three types of displacements may occur, namely: immiscible, multiple-contact miscible and first-contact miscible displacement. Differentiation between these cases(2,3,4) can best be represented on a ternary diagram. For the sake of simplicity, consideration will be given to the case of a three-component hc-system, where C1 represents the light component, C2, the intermediate component and C3, the heavy component. Hence, the phase behaviour of such a system at some fixed pressure and temperature can be rigorously described on a plane ternary diagram.

2.3.1 Immiscible Case.

Suppose that the displacement is conducted at the pressure P1 and temperature T, whereby the displacing fluid is a lean gas (G), while the displaced fluid is an oil (O) relatively rich in the intermediate component, (see Figure 2-A). At the beginning of the displacement, the displacing and displaced fluids are not in thermodynamic equilibrium. Under the influence of the viscous and capillary forces, the displacement will be of the Buckley-Leverett(5) type with the addition of mass transfer between the concurrently flowing phases. The saturation diagram (Figure 2-B) represents an idealized saturation profile in the diphasic

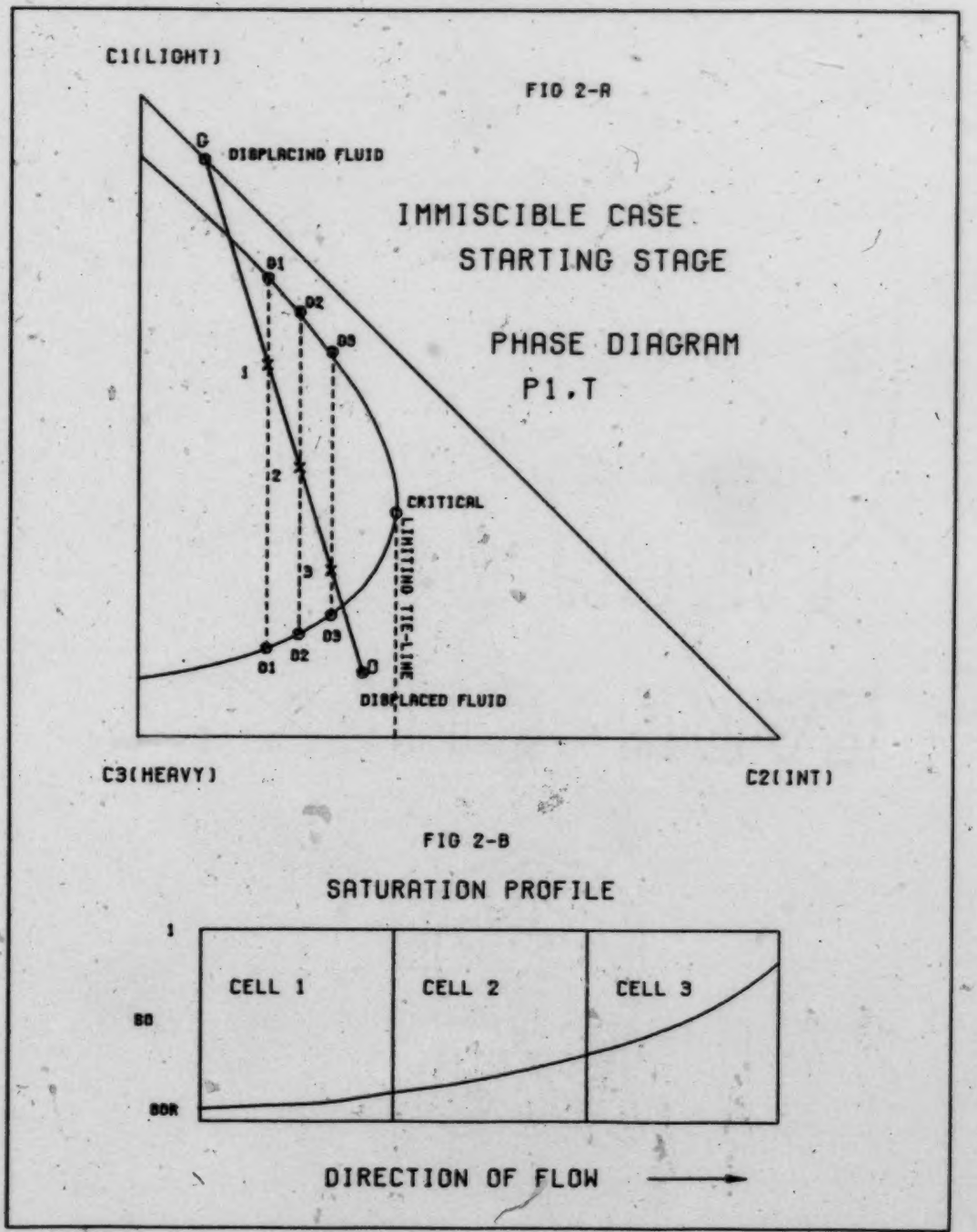
C1(LIGHT)
FIG 2-A
C
DISPLACING FLUID
IMMISCIBLE CASE
STARTING STAGE
PHASE DIAGRAM
P1,T
D1
D2
D3
1
2
3
CRITICAL
LIMITING TIE-LINE
D1
D2
D3
D
DISPLACED FLUID
C3(HEAVY)
C2(INT)
FIG 2-B
SATURATION PROFILE
1
SO
SOR
CELL 1
CELL 2
CELL 3
DIRECTION OF FLOW

zone before thermodynamic equilibrium is established. Let us visualize the porous medium as a series of cells. On this diagram it may be observed that the relative amount of gas to oil decreases going from cell 1 to cell 3. This is reflected on the phase diagram (Figure 2-A) by the overall composition of each cell, namely points 1, 2 and 3. Assuming that thermodynamic equilibrium is established, the composition of each phase in each cell will change. Drawing the tie-lines passing through points 1, 2 and 3 we obtain the following:

cell 1: gas (G1) in equilibrium with oil (O1)

cell 2: gas (G2) in equilibrium with oil (O2)

cell 3: gas (G3) in equilibrium with oil (O3).

Referring to Figure 3-A, as the displacement proceeds, the oil left behind will be contacted by the original displacing lean gas, and will be further stripped of its intermediate component. Its composition path will follow the bubble-point curve, in the direction of lesser intermediate component, until it reaches the limiting composition (OI). This limit is characterized by the particular tie-line passing through (G) and the equilibrium gas (GI). Suppose now that oil (OI) is at the irreducible oil saturation, thus immobile. Oil (OI) will always be in contact with more gas (G). Let (M) be the point representing the overall composition of Ng moles of gas (G) being in contact with Nl moles of oil (OI) before equilibrium is established. From the lever rule, we have:

$$\frac{Ng}{Nl} = \frac{\overline{MOI}}{\overline{MG}} \qquad (2)$$

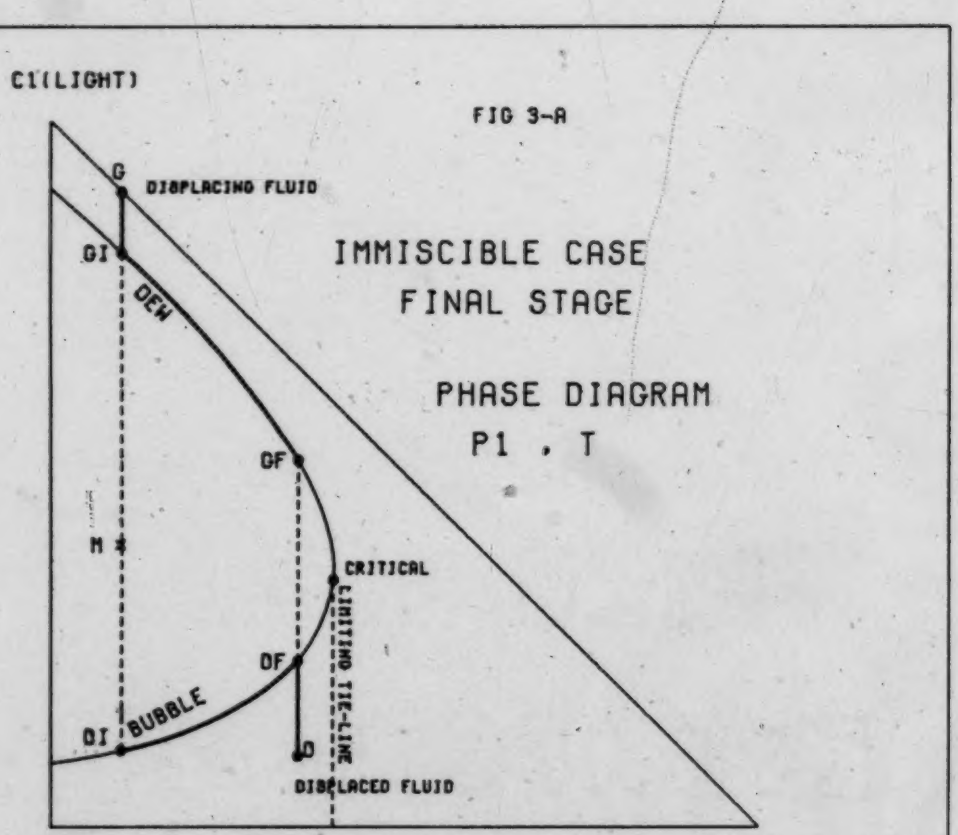

FIG 3-B

SATURATION PROFILE

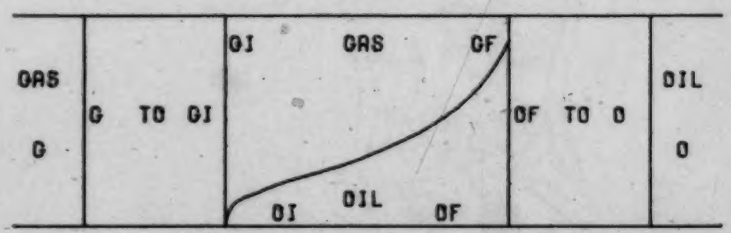

DIRECTION OF FLOW ⟶

At equilibrium, some oil will evaporate and the gas phase composition will change to (GI). The relative amount of gas to oil is therefore changed to:

$$\frac{Ng \text{ equilibrium}}{Nl \text{ equilibrium}} = \frac{\overline{MOI}}{\overline{MGI}} \qquad (3)$$

and Ng equilibrium $>$ Ng, since $\overline{MGI} < \overline{MG}$.

As the oil (OI) is contacted by more lean gas (G), the evaporation process will continue until all the oil has evaporated. This correponds to the evaporation front [1].

Similarly, the gas at the front will contact more virgin oil (O) and becomes more enriched in the intermediate component. Its composition path will follow the dew-point curve, in the direction of higher intermediate component, until it reaches the limiting composition (GF). This limit is characterized by the particular tie-line passing through the original oil (O) and the equilibrium oil (OF). For this case, the saturation distribution as a function of length is illustrated in Figure 3-B and the displacement is clearly immiscible as the gas at the front (GF) is immiscible with the oil being displaced.

---

[1] Note that an evaporation front will exist only if the original displacing gas phase has a composition that does not fall on the dew-point curve. Otherwise a residual oil saturation will always be present.

2.3.2 Multiple-contact Miscible Case (or Dynamic Miscibility).

Suppose now that the displacement is conducted at a higher pressure P2, and at the same temperature T. Any increase of pressure will be followed by a shrinkage of the phase envelope. Let us suppose, as shown in Figure 4-A, that the pressure is high enough so that the same displaced fluid (O) has a composition that places it just to the right of the limiting tie-line.

At the beginning of the displacement, the mechanism is similar to that of the immiscible case, as the line joining point (O) to point (G) crosses the phase envelope (see Figures 4-A and 4-B). This line is the loci of the compositions of all possible combinations of gas (G) and oil (O). Viscous and capillary forces will play the same role and the displacement will be of the Buckley-Leverett type in its starting stage, with the addition of a mass transfer between the concurrently flowing phases. The oil left behind will be contacted by the displacing lean gas (G) and will be stripped further of its intermediate component. Its composition path will follow the bubble-point curve, in the direction of lesser intermediate component, until it reaches the limiting composition (OI) (see Figure 5-A). As discussed earlier, oil (OI) will evaporate in the contacting lean gas (G), until it is completely evaporated. This corresponds to the evaporation front:

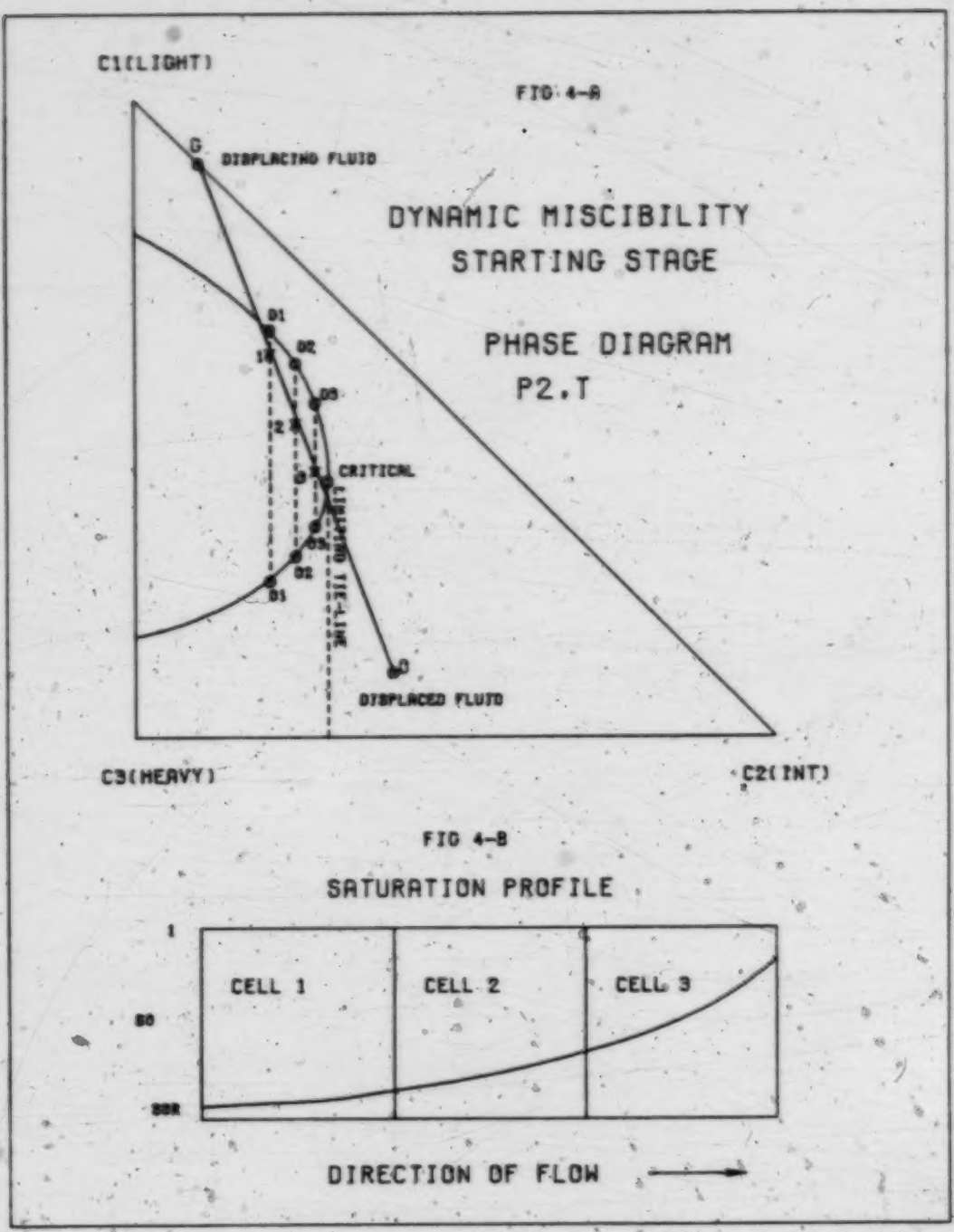
C1(LIGHT)
FIG 4-A
G
DISPLACING FLUID
DYNAMIC MISCIBILITY
STARTING STAGE
PHASE DIAGRAM
P2,T
D1
D2
D3
CRITICAL
D2
D1
D
DISPLACED FLUID
C3(HEAVY)
C2(INT)
FIG 4-B
SATURATION PROFILE
1
CELL 1
CELL 2
CELL 3
DIRECTION OF FLOW

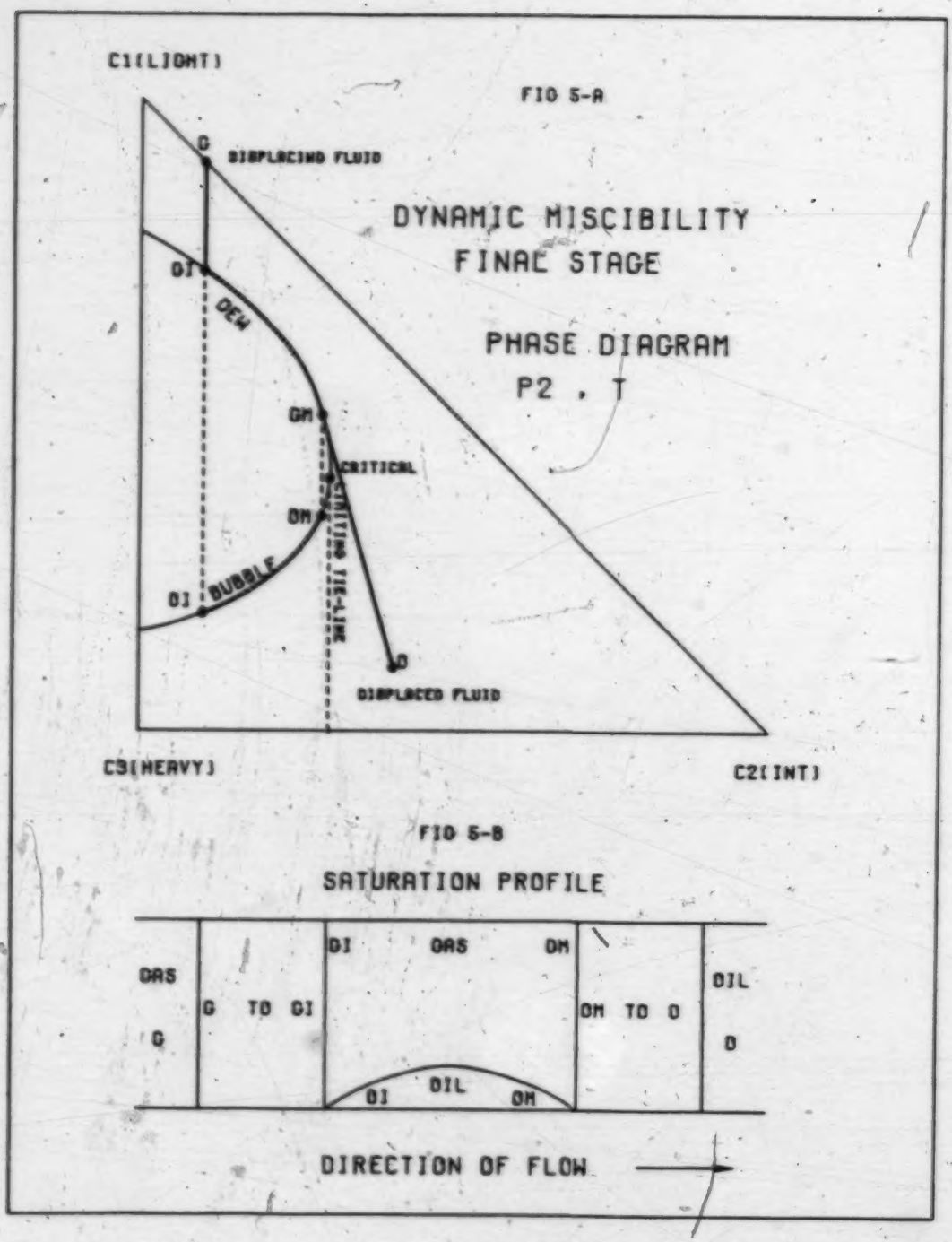
C1(LIGHT)
FIG 5-A
G
DISPLACING FLUID
DYNAMIC MISCIBILITY
FINAL STAGE
PHASE DIAGRAM
P2 , T
OI
DEW
OM
CRITICAL
OM
BUBBLE
OI
DISPLACED FLUID
C3(HEAVY)
C2(INT)
FIG 5-B
SATURATION PROFILE
GAS
G
G TO OI
OI
OIL
OM
GAS
OM TO O
OIL
O
OI
OIL
OM
DIRECTION OF FLOW

Similarly, the gas at the front will contact more virgin oil (O), and thus will further be enriched as the displacement proceeds. Its composition path will follow the dew-point curve in the direction of higher intermediate component, until it reaches the limiting miscibility composition (GM). This limiting composition is characterized by the tangent to the phase envelope passing through point (O). Gas (GM) is now completly miscible with the oil ahead, as the line joining it to point (O) does not cross the phase envelope. At this point, miscibility has been initiated (see Figure 5-B).

Under the influence of dispersion and/or some perturbating phenomena (viscous fingering, gravity override), this displacement will be characterized by the continuous breakdown and reformation of the miscible front. Thus a residual oil saturation will be left behind, resulting in an incomplete displacement of the oil(6). Consider the effect of convective mixing in the gas zone just behind the miscible front (see Figure 5-B). The composition of the different gases forming this zone, falls on the dew-point curve. An explanation of convective mixing is necessary at this point of the discussion. A porous medium may be represented by a bundle of interconnected dissimilar flow channels. Therefore, different interstitial velocities will exist for different flow paths. Consequently gases of different compositions may come in contact, as illustrated by the idealized system shown in Figure 6-A.

IDEALIZED REPRESENTATION OF POROUS MEDIA

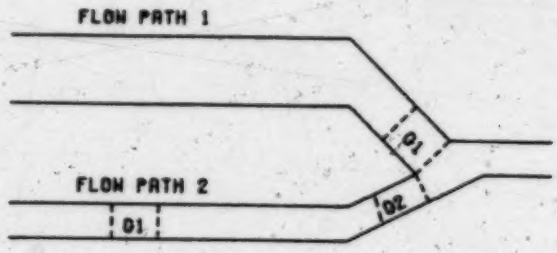

FIG 6-A

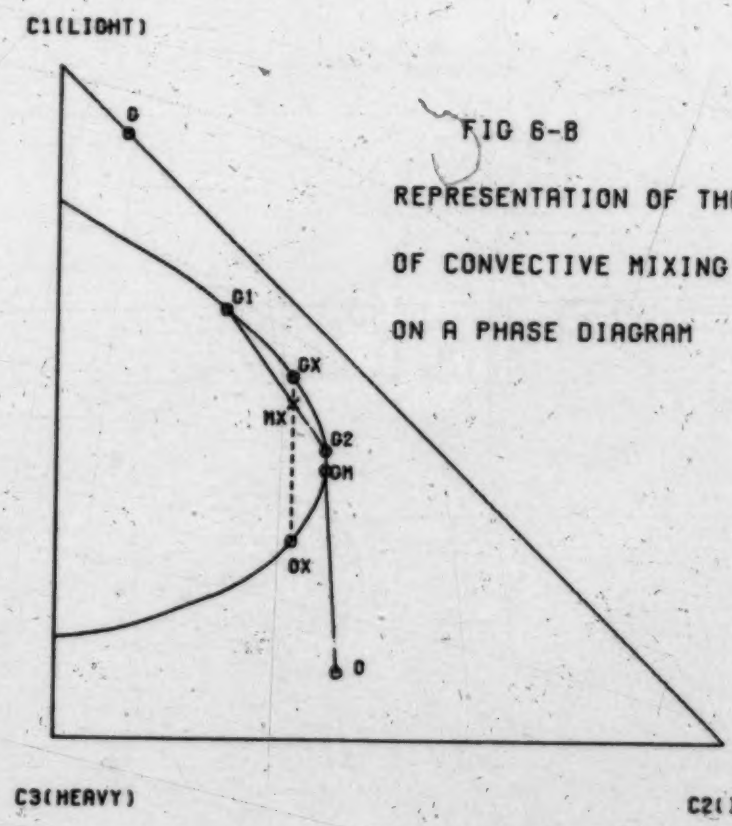

FIG 6-B

REPRESENTATION OF THE EFFECT OF CONVECTIVE MIXING ON A PHASE DIAGRAM

Suppose that leaner gas of composition (G1) travels faster in flow path 1 than richer gas (G2) in flow path 2. At the intersection of the flow paths, gas (G1) may mix with gas (G2), resulting in a mixture of composition (MX) which just falls inside the phase envelope (see Figure 6-B). This will result in the condensation of some oil (OX) which is in equilibrium with gas (GX). This effect is even more pronounced as we increase the injection rate, as the convective portion of dispersion becomes dominant[2]. The same process will disperse the gas of composition (GM) (see Figure 5-B) , resulting in a leaner gas contacting the oil ahead, with the consequent loss of miscibility. Similarly, under the influence of some perturbating phenomena (viscous fingering, gravity override), leaner gas will come into contact with the oil ahead and an immiscible displacement will occur. The same displacement mechanism previously discussed will be repeated with the subsequent reformation of a miscible front.

2.3.3 First-contact Miscible Case.

Suppose now that the displacement is conducted at still a higher pressure P3, and at the same temperature T, and that the shrinkage of the phase envelope is such that the line connecting the points (O) and (G) does not cross the phase envelope (see Figure 7-A). The connecting line (G)-(O) is the loci of all possible compositions encountered

---

[2]The reader may refer to Appendix 1 for a detailed definition and explanation of dispersion in porous media.

in the region where the two fluids are in contact with each other. As this line does not cross the phase envelope, the two fluids are miscible in all proportions (see Figure 7-B). However, the composition path (line (G)-(O)) drawn in Figure 7-A assumes that all the components have the same diffusivity(7). Based on the literature survey, determination of the diffusivities of the different components of a complex hc-system is not an easy task. A detailed procedure for estimating such factors is shown in Appendix 2. The effect of components diffusing with different diffusivities is also treated, with an example, in Appendix 2.

2.4 Definition of the Minimum Miscibility Pressure.

For the vapourizing gas drive just described, the MMP[3] will correspond to the pressure necessary for the limiting tie-line to pass through the point representing the composition of the displaced fluid. The MMP is that pressure below which it is not possible to obtain a dynamic miscible displacement.

Let us consider the case where the displacement is immiscible. Behind the front, a diphasic flow regime will exist, leaving a residual oil saturation. For the case where multiple-contact miscibility is initiated, convective mixing between fluids with compositions lying on the dew-point curve, will result in mixtures which barely fall within the

---

[3]Refer to nomenclature for definition of symbols and terms.

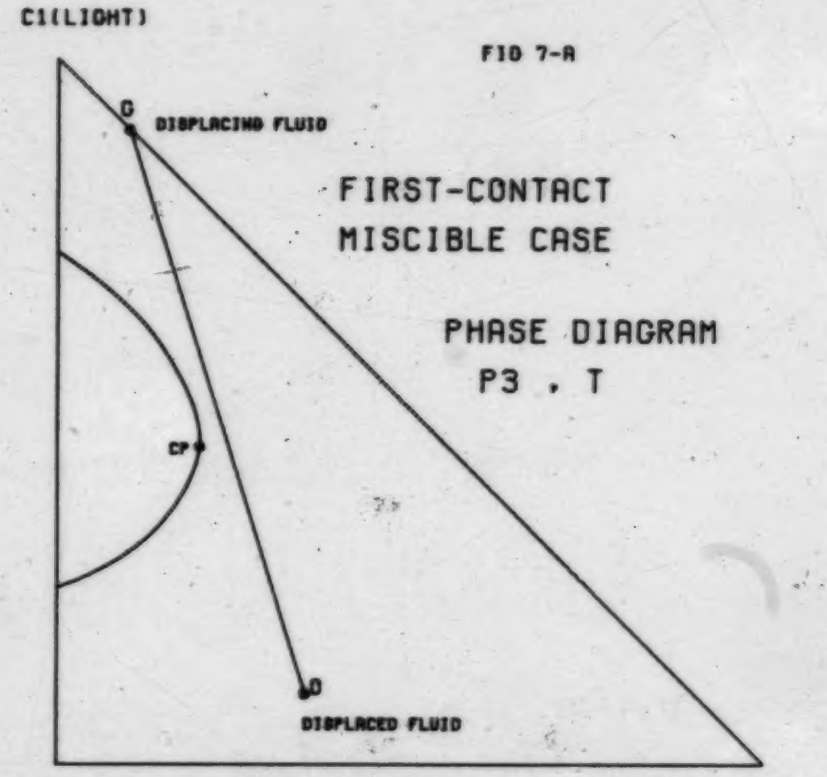
C1(LIGHT)
C
DISPLACING FLUID
FIRST-CONTACT
MISCIBLE CASE
PHASE DIAGRAM
P3 , T
CP
D
DISPLACED FLUID
C3(HEAVY)
C2(INT)

FIG 7-A

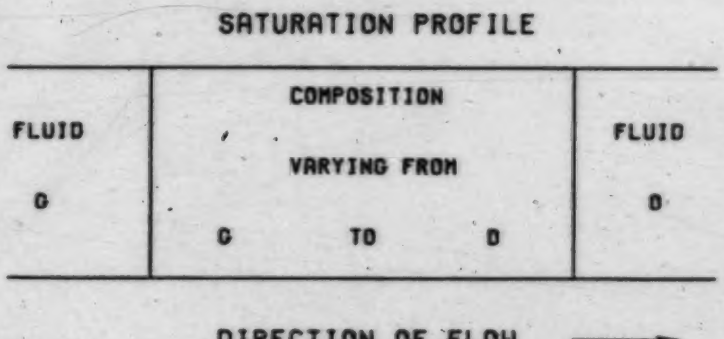
SATURATION PROFILE
FLUID
C
COMPOSITION
VARYING FROM
C TO D
FLUID
D
DIRECTION OF FLOW

FIG 7-B

two-phase region, consequently leaving a small amount of immobile liquid behind the front. Also, any reformation of the miscible front after its breakdown (through dispersion etc...) will be at the cost of even more oil being left behind, though small compared to the amount left behind during an immiscible displacement. This suggests that going from an immiscible to a multiple-contact miscible displacement, will correspond to a sharp decrease in the residual oil saturation at gas breakthrough, or a sharp increase in the recovery of the initial oil in place, and that the overall character of the displacement will change from diphasic to monophasic flow.

Therefore, it follows from the above description that certain basic criteria may be formulated to experimentally determine the MMP. If we plot recovery versus pressure at gas breakthrough, the curve should show a clear break in slope for a value of the pressure greater than or equal to the MMP. Also, if a sight glass is connected to the outlet of the porous medium, the experimenter will observe that the character of the displacement changes from diphasic to monophasic flow for a value of the pressure greater than or equal to the MMP. These are the basic criteria used by the experimenters to define the MMP. The experiments are carried out in an unconsolidated porous medium and the method is referred to as the slim-tube technique.

3. Methods for Estimating the MMP for a Vapourizing Gas Drive

3.1 Introduction.

It may be recalled that the MMP is that minimum pressure necessary to obtain a multiple-contact miscible displacement at constant reservoir temperature for fixed compositions of the resident oil and the injected gas. For the case of a three-component hc-system, which phase behaviour can be rigorously represented on a ternary diagram at some fixed pressure and temperature, the MMP corresponds to the pressure at which the limiting tie-line passes through the point representing the composition of the reservoir fluid.

The MMP can be determined or estimated in three basic ways, namely:

a) pseudo-ternary diagram method

b) windowed PVT-cell method

c) slim-tube test method.

Each of these methods will be described, and their limitations, if any, will be discussed.

An analysis of the slim-tube test method has been the purpose of this research. The investigation pursued will be briefly introduced in this chapter.

3.2 Pseudo-ternary Diagram Method.

This method treats any complex hc-system as being composed of 3 pseudo-components:

the light ends, C1-N2

the intermediates, C2-C6

and the heavy ends, C7+.

Pseudo-ternary diagrams are then constructed at different pressures and constant temperature, based on the NGAA(8) equilibrium constants, under the following assumptions:

a) The light end pseudo-component is of the same composition as the light end fraction of the injected gas.

b) The intermediate and heavy pseudo-components are of the same composition as the intermediate and heavy fractions of the reservoir oil, respectively.

The graphical representation of the phase envelopes associated with each pressure, at constant reservoir temperature, permits the estimation of the MMP. The minimum miscibility pressure is determined by selecting the pressure at which the point representing the composition of the reservoir oil is located just to the right of the limiting tie-line. As previously discussed, any increase in pressure is followed by a shrinkage of the phase envelope. Therefore, if at some pressure the reservoir oil is in the liquid region, an increase in pressure can bring the reservoir oil in the critical region.

There are, however, severe limitations to this approach, as described by Benham *et al.*(9). It has been seen that in the case of a multiple-contact miscible displacement, a transition zone will develop between the original injected gas and the displaced resident oil. Therefore, across the transition zone, the character of the intermediates and heavy-ends groups will vary from that of the injection gas to that of the reservoir oil. Hence, pseudo-ternary diagrams based on the character of these groups in only one of the phases will not describe all the stages involved in obtaining miscibility. Benham *et al.*(9) have suggested a way of overcoming this problem. Although their analysis dealt with the case of a condensing gas drive, the same reasoning can be applied to a vapourizing gas drive. If consideration is limited to the region close to the critical point and the associated tie-line and if it is assumed that the character of the intermediates and heavy-ends of the critical point is close to that of the reservoir fluid, a pseudo-ternary diagram drawn using intermediates and heavy-ends of character equal to that of the reservoir oil will have quantitative significance in the region of the critical point and its associated limiting tie-line.

Also, Hutchinson and Braun(3) have shown that the position of the phase boundary curve on the triangular diagram and the slope of the limiting tie-line depend on the overall composition. The composition cannot be identified by

a C1, C2-C6, and C7+ breakdown, because the components within a pseudo-group have different volatilities. Hence, the character or composition of the pseudo-group will not be the same in coexisting liquid and gas phases.

The problem associated with a phase diagram based on pseudo-components is that it fails to define rigorously the phase relations of a complex hc-system. An examination of the phase rule:

$$F = C - P + 2 \qquad (4)$$

where,

F = degrees of freedom

C = number of components present in the hc-system

P = number of phases,

shows that at constant pressure and temperature, the maximum degrees of freedom equals the number of components present in the hc-system less one.

Consider a four-component hc-system at constant temperature and pressure. From the phase rule, the maximum degrees of freedom is equal to three. Therefore, the phase behaviour of such a system can be rigorously represented on a three-dimensional compositional diagram. This diagram corresponds to a tetrahedron, each apex representing one of the pure components. As opposed to a ternary system, the phase envelope will correspond to a surface. For the sake of clarity, only a portion of this phase envelope is depicted in Figure 8. It may be observed on this figure that different critical mixtures and limiting tie-lines will

FIG 8

PHASE BEHAVIOUR OF A 4-COMPONENT SYSTEM

AT CONSTANT PRESSURE AND TEMPERATURE

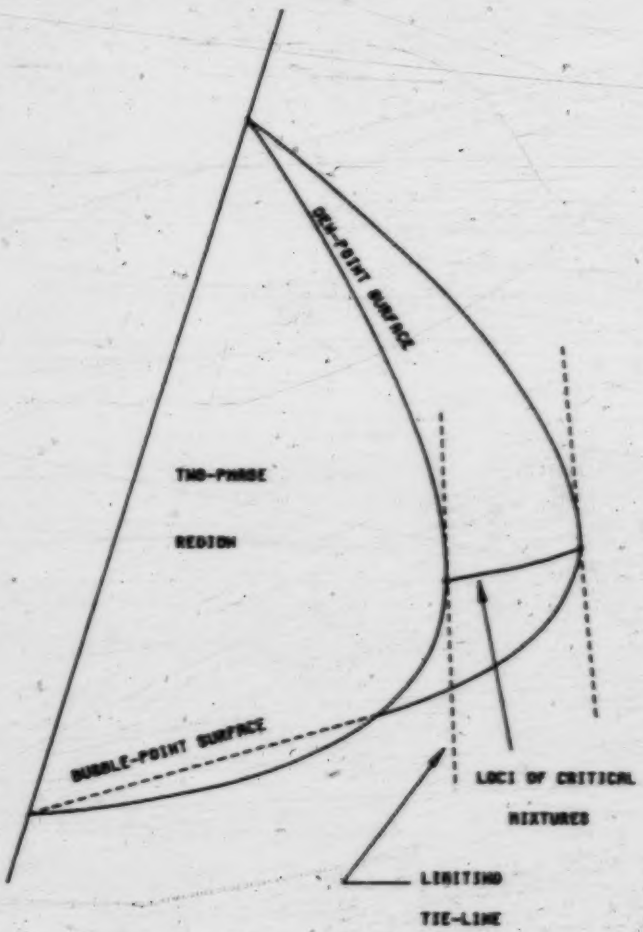

correspond to different sections of the phase envelope. This illustrates the fact that the pseudo-ternary representation of a four-component hc-system (or higher) is quite restrictive. Hence, determination of the MMP based on a pseudo-ternary diagram is only approximate.

3.3 PVT-cell Determination of the MMP.

This method uses a representative sample of the reservoir oil at the desired conditions of pressure and temperature which are maintained constant throughout the batch-contact experiment. A batch-contact experiment involves the establishment of an equilibrium condition between the displacing gas of interest and new original oil within a PVT-cell at some selected pressure and temperature. The procedure consists of a series of repeated experiments at different pressures and constant reservoir temperature, until through an observation of the phases within the cell, one can identify the MMP.

The idea is to duplicate, in a PVT-cell, the enrichment of the gas as it continuously contacts new-original oil, in a vapourizing gas drive. As discussed earlier, two cases are possible:

Immiscible case:

The gas is not enriched enough so as to miscibly displace the oil.

Multiple-contact miscible case:

The gas is sufficiently enriched so as to

miscibly displace the oil.

We will discuss these cases separately, so as to infer what would be the visual observations in a windowed PVT-cell, after n batch-contact experiments, corresponding to each of these cases. A three-component hc-system will be considered, so as to rigorously represent its phase behaviour at some fixed pressure and temperature on a ternary diagram.

3.3.1 The Immiscible Case.

Figure 9 is an illustration of the multiple batch-contact experiment as conducted in a PVT-cell. Suppose that the original reservoir oil and the displacing gas have compositions represented by points (O) and (G), respectively. The PVT-cell is originally filled with oil (O). The first step is to remove some of this oil and to replace it with gas (G) at constant pressure and temperature. At equilibrium, the resulting mixture (M1) (see Figure 9) will separate into two phases, a gas phase (G1) and a liquid phase (O1). The second step is to remove the liquid phase (O1) and to replace it by the original oil (O). At equilibrium, the new resulting mixture (M2) will separate into two phases, a gas phase (G2) and a liquid phase (O2). The second step is then repeated a number of times until at equilibrium the gas phase has a composition (GN) and the liquid phase (ON).

At this point two possibilities may arise:

a) Suppose that the original oil (O) is located on the

FIG 9

REPRESENTATION OF A PVT-CELL MULTIPLE BATCH-CONTACT ON A TERNARY DIAGRAM.

IMMISCIBLE CASE

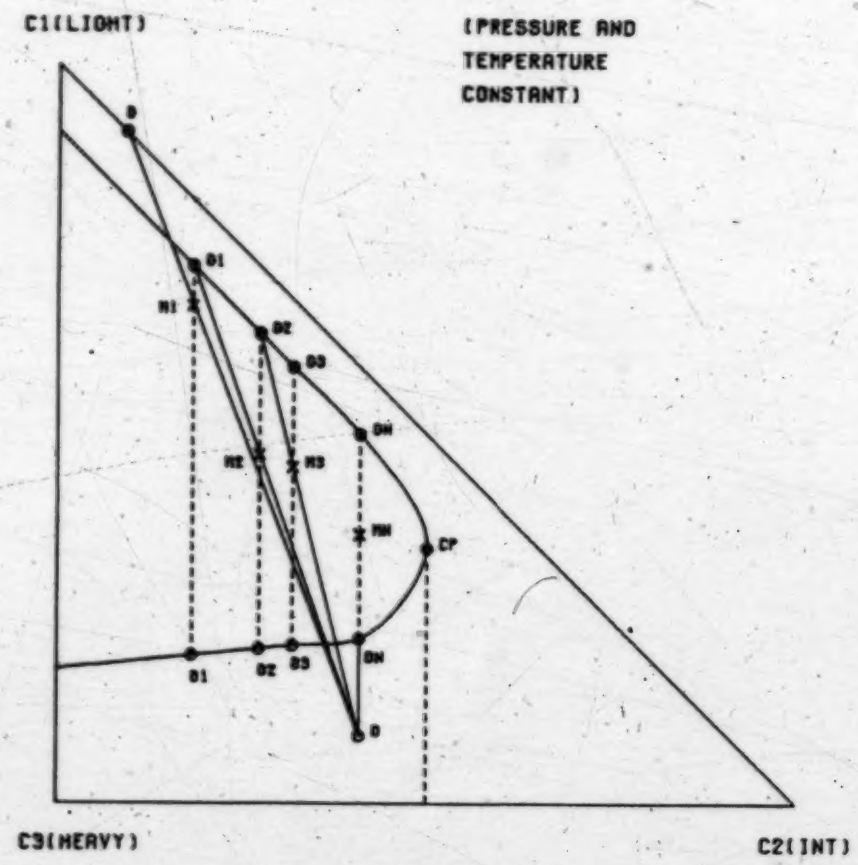

bubble-point curve. One may observe that at the nth stage of the batch-contact experiment, the original oil is in equilibrium with gas (GN). Further replacement of the liquid phase by the original oil will not result in a change of composition of the gas or liquid phases, thus no net mass transfer will occur between these phases as they are in equilibrium. Thus, the saturation of each of the phases in the cell will remain constant.

b) Suppose that the original oil (O) is in the liquid region (as shown in Figure 9). Further replacement of the liquid phase (ON) by oil (O) will result in a change of the overall composition (MN) of the cell, that will follow a path on the tie-line in the direction of point (O). Thus, the liquid saturation of the cell will keep on increasing, ultimately reaching a value of one.

3.3.2 The Multiple-contact Miscible Case.

Proceeding in a manner similar to the previous case, the multiple batch-contact experiment in a PVT-cell for a multiple-contact miscible case is illustrated in Figure 10. Consider the nth step of the multiple batch-contact experiment. At equilibrium the mixture in the cell of overall composition (MN) will separate into two phases, a gas phase (GN) and a liquid phase (ON). Further replacement of the liquid phase (ON) by the original oil (O) will result in an overall mixture (M) which lies on the line tangent to the phase envelope and passing through point (O). Hence, the

FIG 10

REPRESENTATION OF A PVT-CELL MULTIPLE BATCH-CONTACT ON A TERNARY DIAGRAM.

MULTIPLE-CONTACT MISCIBLE CASE

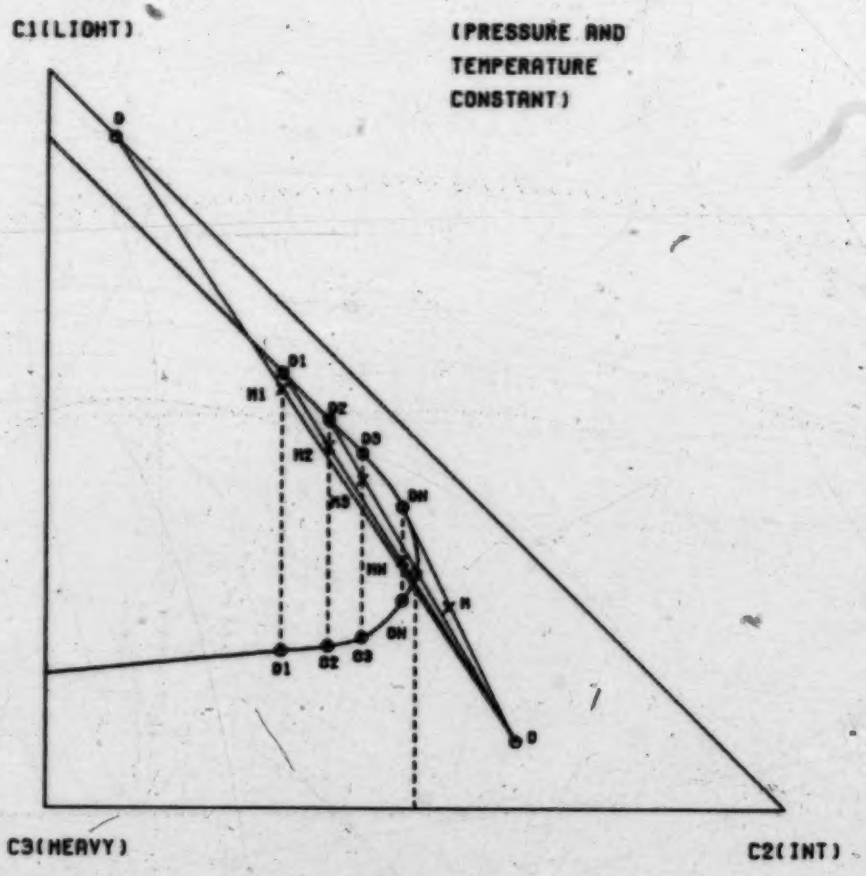

liquid phase will disappear and a single fluid phase will be observed in the windowed PVT-cell.

It may be concluded that after a number of stages in the multiple batch-contact experiment conducted at constant pressure and temperature, two situations are possible:

a) If one observes a constant or increasing liquid saturation in the PVT-cell, the pressure is smaller than the MMP, corresponding to the immiscible case.

b) If, however, a vanishing liquid saturation is observed, the pressure is greater than or equal to the MMP, corresponding to the multiple-contact miscible case.

The MMP will correspond to the minimum pressure for which a vanishing liquid saturation is observed. As can be imagined, the major drawback of this method is that it requires a great deal of time to complete the experiments.

3.4 Slim-tube Test Method.

The minimum reservoir pressure required for the development of a dynamic vapourizing gas miscible drive (MMP) is often determined experimentally by what is referred to as the slim-tube displacement test. In this method, the reservoir oil is displaced with the potential lean gas at constant temperature and at various pressures. The experiments are carried out in an elongated small diameter steel tube packed with glass beads or silica sand.

Before going any further, it is important to note(10,11), that the sand-packed tube displacement apparatus is a device for bringing about multiple contacts between concurrently flowing fluids. It is not intended to simulate reservoir conditions. Hence, slim-tube tests are not indicative of ultimate recovery, macroscopic sweep efficiency, transition zone length, etc..., to be achieved in an actual oil reservoir.

As discussed earlier, the basic criteria defining the MMP rely on the theoretical conclusions that for a value of the pressure greater than or equal to the MMP, an increase in recovery should be observed and that the character of the displacement changes from diphasic to monophasic flow. It is important to note that such criteria will be sound only if the displacement is stable; that is, that the porous medium is evenly swept by the displacing fluid and that any perturbating effects such as viscous fingering and gravity override are suppressed. The results of the literature survey showed that, except for the case of vertical displacements (2,10) where the stability of the displacement is accounted for, none of the other experimental procedures utilized a stability criterion.

Moreover, as observed by Orr *et al.*(1), displacement lengths range from 1.5 to 25.6m, flow geometries vary from vertical to flat coils to spirals, and flow velocities vary over nearly two orders of magnitude. No general consensus exists as to the criteria defining the MMP. These criteria

Table 1

EXPERIMENTAL PROCEDURES and CRITERIA FOR MMP DETERMINATION

Experimenter	Experimental Procedure	Stability Criterion	Criteria Defining MMP
P. Deffrene et al.(2)	Vertical Displacement tube length = 1.5m tube diameter = 0.01m packing material : 60-65 mesh glass beads	Vd < Vc $Vc = Kg \frac{(\rho_2-\rho_1)}{(\mu_2-\mu_1)}$	Plot of recovery vs pressure at gas breakthrough or after 1 to 1.2 PV injection should show a clear break in slope for a value of P = MMP.
Yellig and Metcalfe(11)	Flat coil (Horizontal displacement) tube length = 12.2m tube diameter = 0.457E-2m packing material: 180-200 mesh sand	None Injection rate : 12.2 m/d up to 70% PV inj 24.4 m/d until 1.2 PV inj	Define Miscible displacement as those in which recovery at 1.2 PV was very near maximum recovery obtained in a series of displacements and in which transition-zone fluids appeared in a sight glass. They took as an indication of a multiple contact miscible process, color gradation from dark oil to a yellow fluid. Floods that produced clear vapor and dark oil were judged immiscible.
Holm and Josendal(12)	Flat coil (Horizontal displacement) tube length = 14.6-25.6m tube diameter = 0.472E-2m	None Injection rate: 91.5 m/d	Define miscible diplacements as those that recover more than 80% of the IOIP at gas breakthrough, and that more than 94% of IOIP is recovered ultimately.

are not clearly defined except for those researchers(2,10) who conducted vertical miscible displacements. Table 1 summarizes some of the published experimental procedures and criteria utilized for MMP definition.

Examination of these observations shows that a parametric analysis of the MMP, as determined by the slim-tube test method, was necessary. Thus, the purpose of this investigation was to examine the effect of tube length and injection rate on the displacement efficiency at various pressures covering the immiscible and multiple-contact miscible displacement cases.

4. Stability Considerations in Slim-Tube Displacements

4.1 Introduction.

The experimental work undertaken in this investigation was conducted on a flat slim-tube coil apparatus, as it is the most commonly used in the industry. It may be observed (refer to Table 1) that a stability criterion for displacements carried out on a flat slim-tube coil apparatus (almost a horizontal system) is not utilized. Also, criteria used for MMP estimation by the slim-tube test method are based on recoveries of the IOIP at some arbitrary pore volumes injected of the displacing fluid. It is evident that the method will be influenced by the macroscopic sweep efficiency of the displacement, making it imperative to eliminate the causes for poor sweep. These causes may be different, depending on the displacement type of a vapourizing gas drive.

In the case of immiscible horizontal displacements, poor sweep efficiency is caused by two phenomena:

a) Viscous fingering (viscous forces dominate over capillary and gravity forces).

b) Gravity override (gravity forces dominate).

When the injection rate is sufficiently high, viscous forces, which are proportional to the flow rate, will dominate over the other forces involved in the displacement mechanism. As a result, the displacement will be unstable, with the formation of viscous fingers. Unstable immiscible

displacements are generally characterized by poor macroscopic sweep efficiency, thus lower recoveries at breakthrough of the displacing fluid. If the injection rate is low enough, gravity forces will play a preponderant role provided that the densities of the displaced and displacing fluids are unequal. In this case, a single overriding finger will be formed. Consequently, lower recoveries will be obtain at breakthrough of the displacing fluid. In this type of displacement, capillary forces act as a stabilizing factor. The best sweep efficiency is obtained when the capillary forces are of sufficient magnitude so as to counterbalance the effects of gravity and viscous forces.

On the other hand, for miscible horizontal displacements, poor sweep efficiency is mainly due to gravity segregation at low flow rates. As shown by Crane *et al.(13)*, for high flow rate (all other variables kept constant), the interplay of the diffusive and viscous forces results in a better macroscopic sweep efficiency. If the injection rate is sufficiently high, multiple fingers will be formed, thus increasing the amount the fluids are mixed within the porous medium. Increasing the flow rate results also in an increase of the magnitudé of the diffusive forces, as the dispersion coefficient is a linear function of the flow rate. The multiplicity of the fingers will create a larger contact surface between the displacing and displaced fluids, thus increasing the amount of transverse dispersion which tends to damp out the viscous fingers. An

almost piston-like displacement will result with an improvement in the breakthrough recovery. Therefore, it follows from this preliminary discussion that stability considerations have to be accounted for, if the MMP is to be determined by the flat coil slim-tube test method.

4.2 Stability Considerations for a Vapourizing Gas Drive.

P. Deffrene *et al.*(2) have shown that the MMP is only dependent on the thermodynamic conditions (nature of the fluids and temperature), if proper care is taken to suppress any unstable phenomena, namely viscous fingering and gravity override. They considered a vertical displacement to take advantage of gravity segregation to suppress fingering. The injection rate used was smaller than the critical fingering rate (14) defined as:

$$Vc = Kg \frac{(\rho_2-\rho_1)}{(\mu_2-\mu_1)} \qquad (5)$$

It may be observed that Equation (5) applies only if the displacement is of the first-contact miscible type or when dynamic miscibility has been initiated. As discussed earlier, a multiple-contact miscible displacement will generally start off as an immiscible displacement. It appears then that a different criterion should used during the immiscible portion of the displacement.

Before proposing a possible criterion, let us study more closely the instability phenomena. When one fluid

displaces another of different properties in a homogeneous porous medium, several factors may influence the efficiency of the displacement. These include:

a) mobility ratio

b) displacement rate

c) gravity segregation

d) model dimensions.

Assuming equal densities for the displacing and displaced fluids: In an immiscible displacement, with a mobility ratio greater than unity, instability or viscous fingering will occur when the capillary forces are not large enough to render saturations uniform transversally to the direction of flow. In other words, the viscous and capillary forces will be unbalanced. Similarly, for a miscible displacement with mobility ratio greater than unity, instability will occur when dispersion is of insufficient magnitude to render concentrations uniform transversally to the direction of flow. In this case, the viscous and diffusive forces will be unbalanced. For the case where the fluids have different densities, the effect of gravity can be beneficial or detrimental depending on the relative positions of the displaced and displacing fluids, the displacement rate, the mobility ratio and the angle of dip.

The existence of a critical rate has been discussed by C. Marle (15) (a similar treatment by Hawthorne (16) is also available). A sharp interface between the fluids is assumed, neglecting then the effect of the transition zone which

exists across the interface. Implicit in this approach is the assumption that the stabilizing effect of the capillary and diffusive forces on immiscible and miscible displacements, respectively, can be neglected. Only the interaction of the viscous and gravity forces is taken into account. Consider the case of a one dimensional flow (see Figure 11), whereby fluid 1 or fluid 2 may be the displacing fluid, and let us adopt the following conventions:
Vd is positive, if it is in the same direction as vector $\vec{E}$.
θ is negative, if $\vec{E}$ is directed downward.
Let,

$$Vc = Kg \frac{(\rho_1 - \rho_2) \sin \theta}{\mu_1/Kr_1 - \mu_2/Kr_2} \tag{6}$$

$$M = \frac{K_1 \mu_2}{K_2 \mu_1} \tag{7}$$

$$\frac{\mu_1}{K_1} (M - 1) (Vd - Vc) \tag{8}$$

If the sign of Equation (8) is negative, the interface between the fluids is stationary (remains unchanged with time) and the displacement is stable or subcritical. If the sign of Equation (8) is positive, the interface between the fluids is non-stationary and the displacement is unstable or supercritical.

It may be observed that the relative permeabilities (Kr1 and

FIG 11

RELATIVE POSITIONS OF FLUID1 AND FLUID2

AS RELATED TO THE CONVENTIONS ADOPTED

IN THE STATEMENT OF EQUATIONS (8) AND (8)

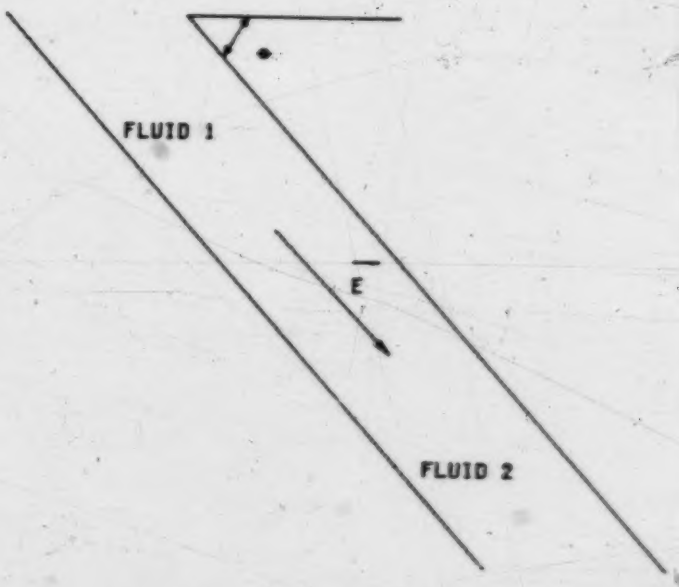

Kr2) in Equation (6) become unity in the case of a miscible displacement.

Consider the case of a vapourizing multiple-contact miscible displacement conducted in a vertical slim-tube, where a more mobile, lower density gas (fluid 1) is displacing a less mobile, denser oil (fluid 2). The mobility ratio (ratio of displacing to displaced fluid mobilities) is therefore greater than unity. The stability criterion for the immiscible portion of the displacement will be given by:

$$Vd \leq Vc\text{-immiscible} \quad \text{and} \quad Vc\text{-immiscible} = Kg\frac{(\rho_2-\rho_1)}{(\mu_2-\mu_1/Kr_1)} \qquad (9)$$

(Kr2=1 since the tube is initially saturated with fluid 2) The corresponding criterion for the miscible portion of the displacement will be given by:

$$Vd \leq Vc\text{-miscible} \quad \text{and} \quad Vc\text{-miscible} = Kg\frac{(\rho_2-\rho_1)}{(\mu_2-\mu_1)} \qquad (10)$$

An examination of Equations (9) and (10) shows that Vc-immiscible is smaller than Vc-miscible. This suggests then that the displacement should be conducted at a lower rate during the immiscible portion of the displacement. The injection rate could then be increased, once dynamic miscibility is initiated, within the limit imposed by Equation (10). For vertical displacements, the assumption of neglecting the effect of the transition zone is not very restrictive as high permeability and very low gas-oil

capillary pressure in the diphasic zone behind the front, allow the gravity forces to control the displacement and limit the length of the transition zone.

The above statement, however, does not hold for the case of displacements conducted in flat slim-tube coils, which are nearly horizontal. An examination of Equations (6) and (8) shows that for $\theta=0$ the displacement will always be supercritical if the mobility ratio is greater than unity. In this case, the gravity forces act and tend to segregate the fluids perpendicularly to the direction of flow, resulting in a wider transition zone. The criteria defined in Equations (6) and (8) can no longer be utilized, as they are based only on the interaction of the viscous and gravity forces. When these forces are orthogonal to each other, the effect of one force can be used to alter the effect of the other on the displacement. In order to define similar criteria for horizontal systems, it is imperative to include the effect of the capillary and diffusive forces for immiscible and miscible displacements, respectively. The following discussion will summarize some of the findings on stability of immiscible and miscible displacements in horizontal systems, based on the literature survey. Some conclusions will be inferred, as to the applicability of these findings to the case of a vapourizing gas drive conducted on a flat slim-tube coil.

4.3 Onset of Instability During Two-phase Immiscible Displacement.

A dimensionless number and its critical value for predicting the onset of instability during two-phase immiscible displacement in porous media has been proposed by Peters and Flock(17). Although their analysis dealt with an oil-water system, it will be assumed that the method can be applied to a gas-oil system. In this case, the oil will be the wetting phase and the gas, the non-wetting phase. The dimensionless number, for cylindrical systems, is given by:

$$Isc = \frac{V(M-1-Ng)\mu gD^2}{C^*\sigma Kgor} \qquad (11)$$

Where,

$$Ng = \frac{Kgor(\rho g-\rho o)g\cos\alpha}{\mu gV} \qquad (12)$$

and

$$M = \frac{Kgor}{\mu g}\,\frac{\mu o}{Kogr} \qquad (13)$$

As the slim-tube is initially saturated with oil, and the system is horizontal, it follows that:

$$M = \frac{Kgor}{\mu g}\,\frac{\mu o}{K} \qquad (14)$$

and

$$Isc = \frac{V(M-1)\mu gD^2}{C^*\sigma Kgor} \qquad (15)$$

For stable displacement in cylindrical systems, the following condition must be met:

$$Isc < 13.56 \qquad (16)$$

Above the limiting value of 13.56 for Isc, the displacement becomes unstable, resulting in lower recovery at breakthrough of the displacing phase.

The expression of the dimensionless number (Isc), provides some hints on how to design or alter the physical characteristics of the porous medium, in order to insure the stability of an immiscible horizontal displacement. The fluid properties (viscosity) and the interfacial tension being fixed, the criterion for stability can be met by altering certain parameters as follows:

a) a decrease of the tube diameter

b) an increase of the intrinsic permeability of the porous medium

c) a decrease of the superficial velocity.

In the case of an immiscible vapourizing gas displacement (or during the immiscible portion of a multiple-contact miscible displacement), mass transfer between the phases will have a beneficial effect as the interface mobility ratio is reduced. However, it will also lower the interfacial tension, resulting in a decrease of the magnitude of the capillary forces. If we assume that the decrease in mobility ratio counterbalances the decrease in interfacial tension, the ratio $(M-1)/\sigma$ of Equation (15) becomes a constant which can be evaluated at the initial

conditions, as if no mass transfer has occurred between the phases. Given the physical characteristics of the porous medium and the fluid properties, Equations (15) and (16) permit the setting of an upper bound on the superficial velocity, in order to ensure the stability of the displacement:

$$V \leq \frac{13.56\ C^{*}\ \sigma\ K_{gor}}{(M-1)\ \mu_g\ D^2} \qquad (17)$$

For a multiple-contact miscible horizontal displacement conducted at a superficial velocity greater than the critical rate of Equation (17), longer travel length for the displacing phase will be required before full miscibility is achieved. Viscous fingers will tend to disperse the miscible front, and will widen the transition zone. The increase in size of the transition zone has a beneficial effect as a gradual change in the mobility ratio is obtained across the diphasic zone. However, before full miscibility is achieved, the transition zone has to be of sufficient size which implies a longer travel distance of the displacing phase in the slim-tube. This will result in an increase in the amount of oil left behind during the immiscible portion of the displacement, thus a lower overall recovery.

4.4 Stability Considerations of Miscible Displacements.

Miscible displacements are characterized by the interplay of three forces, namely:

a) gravity forces

b) viscous forces

c) diffusive forces.

Several researchers studied the interaction of these forces. Crane *et al.*(13) considered the viscous and gravity forces (although the diffusive forces were implicitly included). Their experimental work dealt with the effect on recovery of the mobility ratio and the viscous/gravity forces ratio in a linear horizontal miscible displacement. This ratio included the length/width ratio of the model studied. For a given mobility ratio, they observed that four flow regimes are possible, depending on the viscous/gravity forces ratio. Their results are illustrated in Figure 12 (after F.I. Stalkup (18)). At very low values of the viscous/gravity forces ratio, the displacement is characterized by a single gravity finger (Region 1). In this region breakthrough recovery increases as the viscous/gravity forces ratio increases. At higher values of the viscous/gravity forces ratio (Region 2), the breakthrough recovery is independent of the ratio until a critical value, which depends on the mobility ratio, is exceeded. Beyond this critical value, a transition zone is encountered (Region 3), where secondary fingers form beneath the main gravity finger. In this region, the recovery increases sharply with increasing

FIG 12

FLOW REGIMES IN A TWO-DIMENSIONAL,

UNIFORM LINEAR SYSTEM

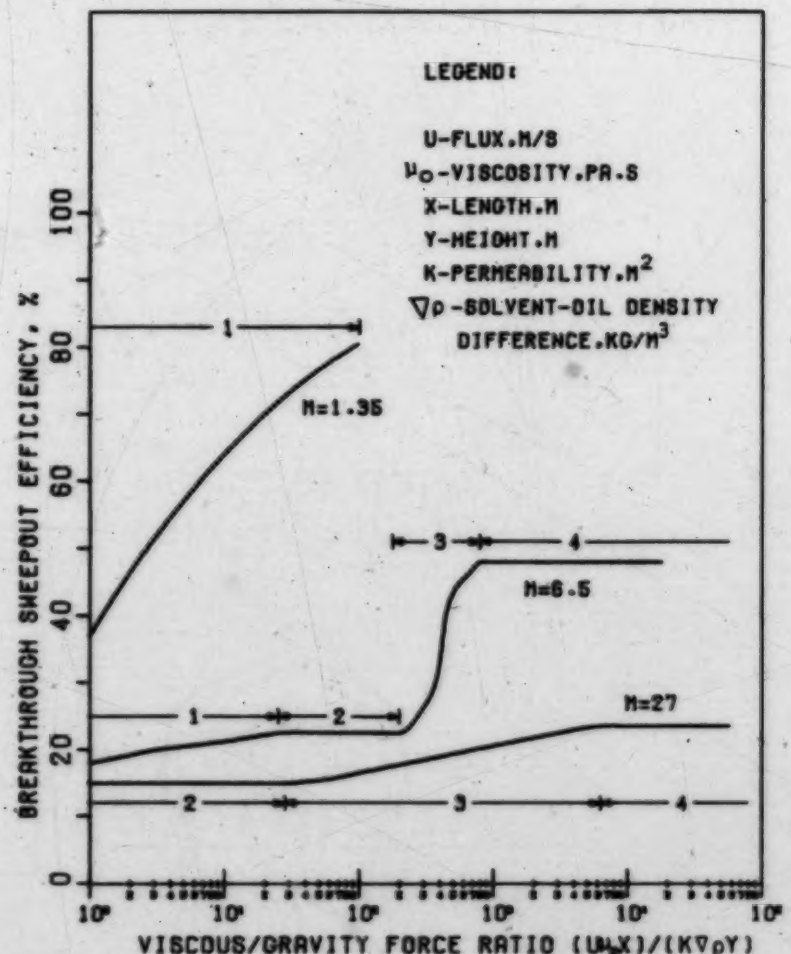

values of the viscous/gravity forces ratio. Beyond the transition zone, the displacement is entirely dominated by viscous fingers and the breaktrough recovery again becomes independent of the viscous/gravity forces ratio (Region 4). They observed that, in any region, the breaktrough recovery decreases as the mobility ratio increases. It appears then that for horizontal miscible floods, displacement by viscous fingering is the most efficient mechanism.

Blackwell(19) studied the case where the displacing and displaced fluids were of equal density. His work was an extension of Crane *et al.*(13) study, as the viscous/gravity forces ratio was infinity. His experimental work dealt with the interaction of the viscous and diffusive forces, when the displacement was by viscous fingering. The parameters studied were the injection rate, model dimensions and the mobility ratio for a linear horizontal miscible displacement. The results of his investigation as to the effect of each of the above parameters showed that:

Effect of model dimensions:

For a given injection rate and mobility ratio, the breakthrough recovery increases as the length/width ratio increases. In all models, fingers, formed in the initial stage of the displacement, are damped out by lateral dispersion. For both narrow and wide models, a transition zone is formed with a gradual change in viscosity from the displacing to the displaced fluid, which minimized the initiation of additional fingers.

resulting in an almost piston-like displacement. This transition zone was formed sooner for narrow models than it was for wider models. For different model dimensions, but equal length/width ratio, the observed cumulative recoveries were identical. The relative length of the transition zone, with respect to the model length, was larger for the smallest model.

Effect of injection rate:

For given model dimensions and mobility ratio, his investigation showed that the higher the rate of flow, the longer the travel length of the displacing fluid before the transition zone was formed. The size of the zone increased with an increase of the injection rate.

Effect of mobility ratio:

He observed that, while early breakthrough of the displacing fluid is obtained when the mobility ratio is high, a considerable incremental recovery is obtained after breakthrough. For instance, for a mobility ratio of 375, the breakthrough recovery was only 14%, while the recovery reached 45% after one pore volume injection. Also the smaller the mobility ratio, the sooner the stabilization of the displacement with the formation of a transition zone.

It appears then that miscible displacements above a critical fingering rate, become stabilized for all model dimensions and rates when the transition zone is formed. This stabilization occurs sooner for narrow models and for lower

injection rate and lower mobility ratio.

The same general results were reported by Van Der Poel (20) who studied the effect of lateral dispersion on miscible displacement in horizontal systems. The results of his investigation showed that:

a) In a horizontal system, a lower density displacing fluid tends to override the higher density resident fluid in the shape of a tongue as a result of gravity segregation at low injection rates.

b) In a narrow model (laboratory model), the mixing zone width across the tilted interface is of a size comparable to the lateral dimension of the model.

c) At low injection rates, the gravity forces play a dominant role compared to the transversal dispersion, resulting in a pronounced gravity tongue and consequently a low recovery at breakthrough.

d) At high injection rates, gravity forces played a lesser role and convective mixing was dominant. This resulted in an almost piston-like displacement with a wider mixing zone and higher recovery at breakthrough.

Based on these findings, it may be assumed then that miscible displacement by viscous fingering in laboratory models is the most efficient mechanism of recovery.

Consider the case of a multiple-contact miscible vapourizing gas displacement in a horizontal slim-tube. In its approach towards miscibility a transition zone (diphasic zone) would have already been created. Increasing the injection rate, as

to promote viscous fingering, will result then in a more piston-like displacement, with increased breakthrough recovery. Stabilization , with the formation a transition zone mutually miscible with the enriched gas at the front and the displaced fluid, will occur rapidly due to the nature of the model. The displacements are indeed carried out in narrow models with length/width ratio as high as 5000 (core diameter of the order of 0.5cm), when the MMP is determined by the slim-tube technique. However, at high rates, there will be an adverse effect due to increasing convective mixing in the gas phase, resulting in the condensation of more immobile oil which will be left behind the front.

4.5 Applications to Vapourizing Gas Displacements Conducted in Horizontal Slim-tubes.

For the case of a vapourizing gas drive in horizontal slim-tubes, several conclusions may be inferred from this discussion. As discussed earlier, one of the criteria used in the determination of the MMP is based on the relationship between the recovery of the IOIP at 1. to 1.2 pore volumes injection and the operating pressure. The idea is to distinguish between immiscible and multiple-contact miscible displacements in terms of recoveries.

From the discussion on the onset of instability during two-phase immiscible horizontal displacement, immiscible vapourizing gas displacements conducted at rates above a

critical fingering rate will result in lower recoveries at breakthrough of the displacing phase. In the case of multiple-contact miscible vapourizing gas floods, displacements by viscous fingering will result in a more efficient sweep efficiency once miscibility has been initiated. However, the length of the tube immiscibly displaced, necessary for miscibility to be dynamically created, will be longer. If the length of the slim-tube is sufficiently long, so as to minimize the length of immiscible displacement with respect to the total system length in the case of a multiple-contact miscible displacement, the following conclusions may be drawn:

a) displacement of immiscible vapourizing gas drives by viscous fingering will result in lower recoveries

b) displacement of multiple-contact vapourizing gas drives by viscous fingering will result in higher recoveries.

It appears then that a better differentiation between immiscible and multiple-contact miscible vapourizing gas drives, as conducted in flat coil slim-tubes, is obtained when the displacement is dominated by viscous fingering. Therefore, if the MMP is to be determined by the flat coil slim-tube technique, one should use as an additional criterion that promoting viscous fingering by increasing the injection rate above a critical value will accentuate the break in slope of the recovery versus pressure curve for a value of the pressure greater than or equal to the MMP. Also

increasing the length of the system will more clearly define the break in slope.

5. Experimental Apparatus and Experimental Procedure

5.1 Description of the Slim-tube Apparatus.

The apparatus (see Figure 13) is composed of:

a) An injection system which permits displacement at constant injection rate.

b) An unconsolidated porous medium (slim-tube).

c) A sight glass (observation of the transition zone).

d) A metering valve (continuous downstream pressure control).

e) A separator at atmospheric conditions, a condenser and metering devices for the liquid and gaseous phases.

f) A gas chromatograph (analysis of the effluent gas).

A Ruska positive displacement pump was used as the injection system. This pump was of the double-cylinder type and was geared for discharge rates of from 10 to 1200 cc per hour per cylinder and calibrated to 0.01cc.

The slim-tube utilized was of variable length. It consisted of a series of interconnected 6.1m long, 0.635cm OD stainless steel tubes. The tubes were dry packed with 100-150 mesh glass beads in a vertical position, before being coiled. This procedure was used as a result of some communication with the technical services of D. B. Robinson and Associates Laboratory (Edmonton). Packing a pre-coiled tube necessitated a vibrating table which induced stress cracking of the steel tube. A 250 mesh sintered steel filter was placed at each end of the tube and maintained in place

FIG 13

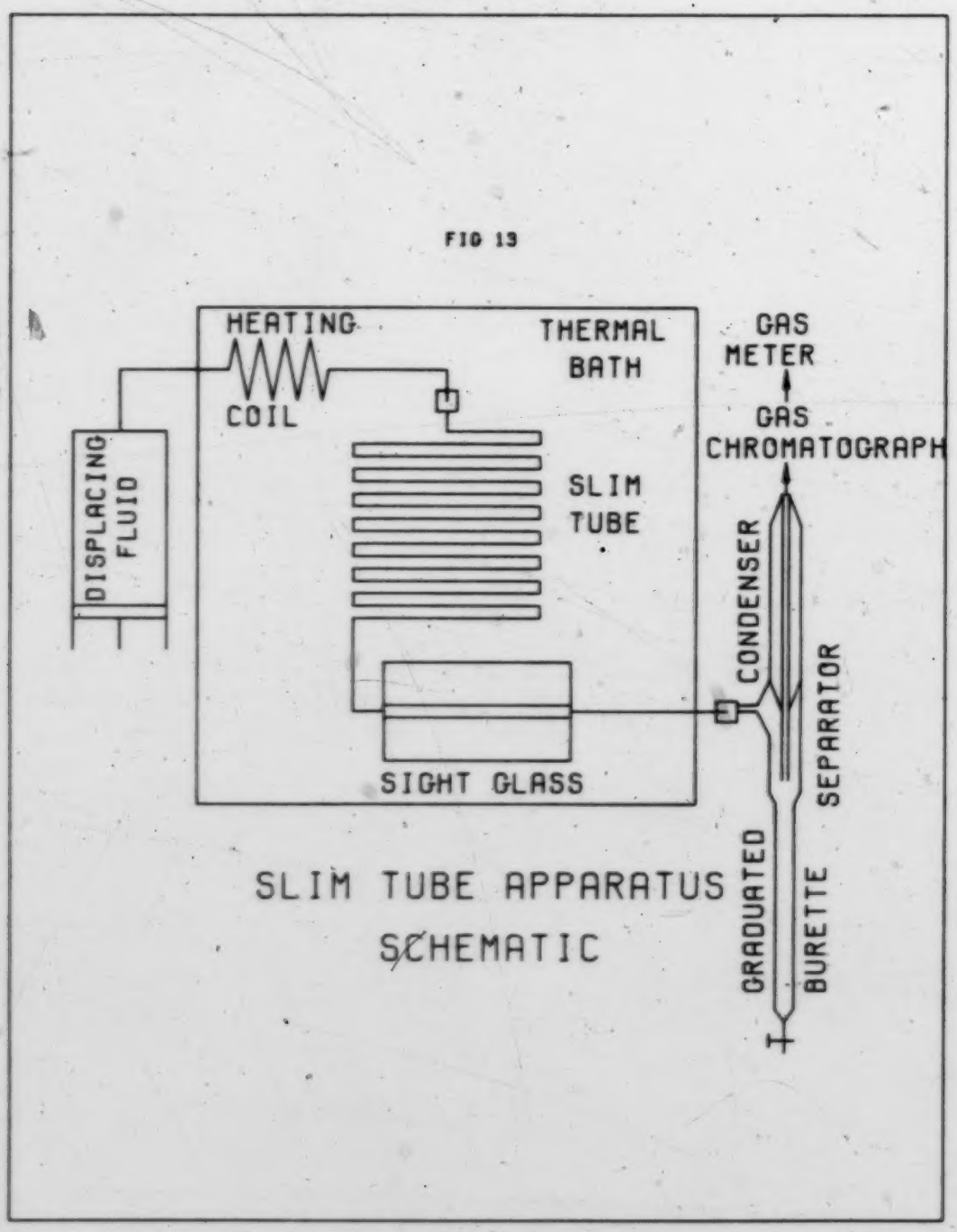

SLIM TUBE APPARATUS

SCHEMATIC

by a washer and a 0.635cm fitting. Each tube was then evacuated for a period of 24 hours before being saturated with distilled water, while a vacuum was maintained at the downstream end. After breakthrough of the water, the vacuum pump was disengaged and a further four pore volumes of water were injected prior to measurements leading to the determination of the liquid permeability. The porosity was determined by the gravimetric method, given the wet weight (saturated tube), dry weight and dimensions of the tube. The tubes were subsequently dried in an oven for a period of 48 hours. The slim-tube physical characteristics are presented in Table 2:

Table 2

Slim-tube Physical Characteristics

Core No	Length (m)	ID (m)	Porosity (%)	Liquid Permea-bility (m^2)
1	6.1	0.457E-2	37.83	10.82E-12
2	6.1	0.457E-2	37.44	09.50E-12
3	6.1	0.457E-2	36.81	10.82E-12

A high pressure sight glass was connected to the downstream end of the slim-tube. It allowed for the

observation of the effluent at the operating conditions of pressure and temperature of the displacement. The slim-tube and sight glass were enclosed in constant temperature air bath.

A 5830 A Hewlett Packard gas chromatograph was used for the analysis of the effluent gas, and chromatograms were obtained every 20 minutes.

Initially a back-pressure regulator was used for downstream pressure control. However, use of this device resulted in pulsating fluid production and about 400 kpa fluctuations of the downstream pressure. It was subsequently replaced by a high pressure fine metering valve which permitted a continuous fluid production, and the downstream pressure was maintained within 50 Kpa of the set value.

5.2 Experimental Procedure.

For each test conducted, the displaced oil was composed of n-butane and n-decane with a composition fixed at 64 mole% and 36 mole%, respectively (it will be subsequently referred to as the live oil). N-decane (99% minimum purity) was purchased from Fischer Scientific Ltd (Edmonton). N-butane (99.5% minimum purity) was purchased from Matheson Ltd (Edmonton). The n-butane - n-decane mixture was prepared by Matheson Ltd. The Mixture was stored in a cylinder and maintained in a single liquid phase under a pressure of 1380 kpa by means of a helium blanket. The displacing fluid was methane. Technical methane (98% minimum purity) was

purchased from Matheson Ltd.

Prior to the initiation of a displacement, the slim-tube apparatus was thoroughly checked for leaks, then evacuated for 20 hours. The coil was saturated with toluene at the desired test temperature and pressure. The toluene was subsequently displaced with the live oil at the same operating conditions. Approximately 3 pore volumes of live oil were injected. This saturation procedure was used in order to prevent phase separation of the live oil, the test pressure always being above its bubble-point pressure. The system was then allowed to equilibrate at the test temperature overnight. The pressure of the displacing fluid was brought to the desired test pressure. The displacing fluid was allowed to equilibrate at the test temperature in the heating coil upstream of the slim-tube inlet, during which displacing and displaced fluids were isolated by a valve. At equilibrium, the displacement proceeded at the desired injection rate, while the downstream pressure was continuously monitored by adjusting the metering valve. The effluent was flashed to atmospheric conditions, and the separator gas flow rate and liquid volume were recorded with time, using a bubble flow meter and a 100cc graduated burette. In addition, the separator gas was analysed with a chromatograph every 20 minutes. The transition zone was monitored by observing the phase conditions of the effluent as it flowed in the high pressure sight glass. The observations of the transition zone effluent were noted.

After two pore volumes of the displacing gas were injected, the test was terminated.

For the purposes of calculating the recovery of the IOIP versus the pore volume injected, the following calculations were necessary. The amount of the gas phase injected was obtained using the real gas law:

$$VH = \frac{(P \cdot Vr) \ / \ (Zr \cdot Tr)}{P \ / \ (ZH \cdot TH)} = \frac{ZH \cdot TH}{Zr \cdot Tr} \ Vr \qquad (18)$$

where,

TH = test temperature, K°

Tr = room temperature, K°

P = test pressure (constant throughout the test), Kpa

Vr = volume of gas displaced from the external gas cylinder at Tr and P, m^3

VH = volume of gas injected at TH and P, (accounts for thermal expansion in the temperature bath), m^3

Zr = compressibility of methane at P and Tr

ZH = compressibility of methane at P and TH

The compressibilities for methane were obtained from reference (21).

The volume of oil displaced at test temperature and pressure was calculated by multiplying the produced separator liquid volume by a predetermined volume factor (VF):

$$\% \text{ Recovery of IOIP} = \frac{(\text{Separator Liq Volume}) \times VF}{\text{Pore Volume}} \times 100 \qquad (19)$$

This factor was calculated from a knowledge of the phase and volumetric behaviour of the n-butane - n-decane system at atmospheric conditions and at test temperature and pressure(22). The compositions of the dead oil (separator liquid of a flashed live oil at atmospheric conditions) and liberated gas at atmospheric conditions (see Figure 14) showed that the gas phase was mainly composed of butane and that virtually no decane was present.

Therefore, a material balance on n-decane was performed and the volume factor (VF) was found to be:

$$VF = \frac{Vl}{Vd} = \frac{X10d}{X10l} \cdot \frac{\overline{Vl}}{\overline{Vd}} \qquad (20)$$

where,

X10l = mole fraction of decane in live oil (0.36)

X10d = mole fraction of decane in dead oil (0.545 from Figure 13)

$\overline{Vl}$ = molar volume of live oil at test pressure and temperature, m^3/gmole

$\overline{Vd}$ = molar volume of dead oil at atmospheric conditions, m^3/gmole

Vl = volume of oil at test pressure and temperature, m^3

Vd = liquid volume when Vl is flashed to atmospheric conditions, m^3

It may be observed that this method assumed that after breakthrough of the displacing fluid, the liquid produced

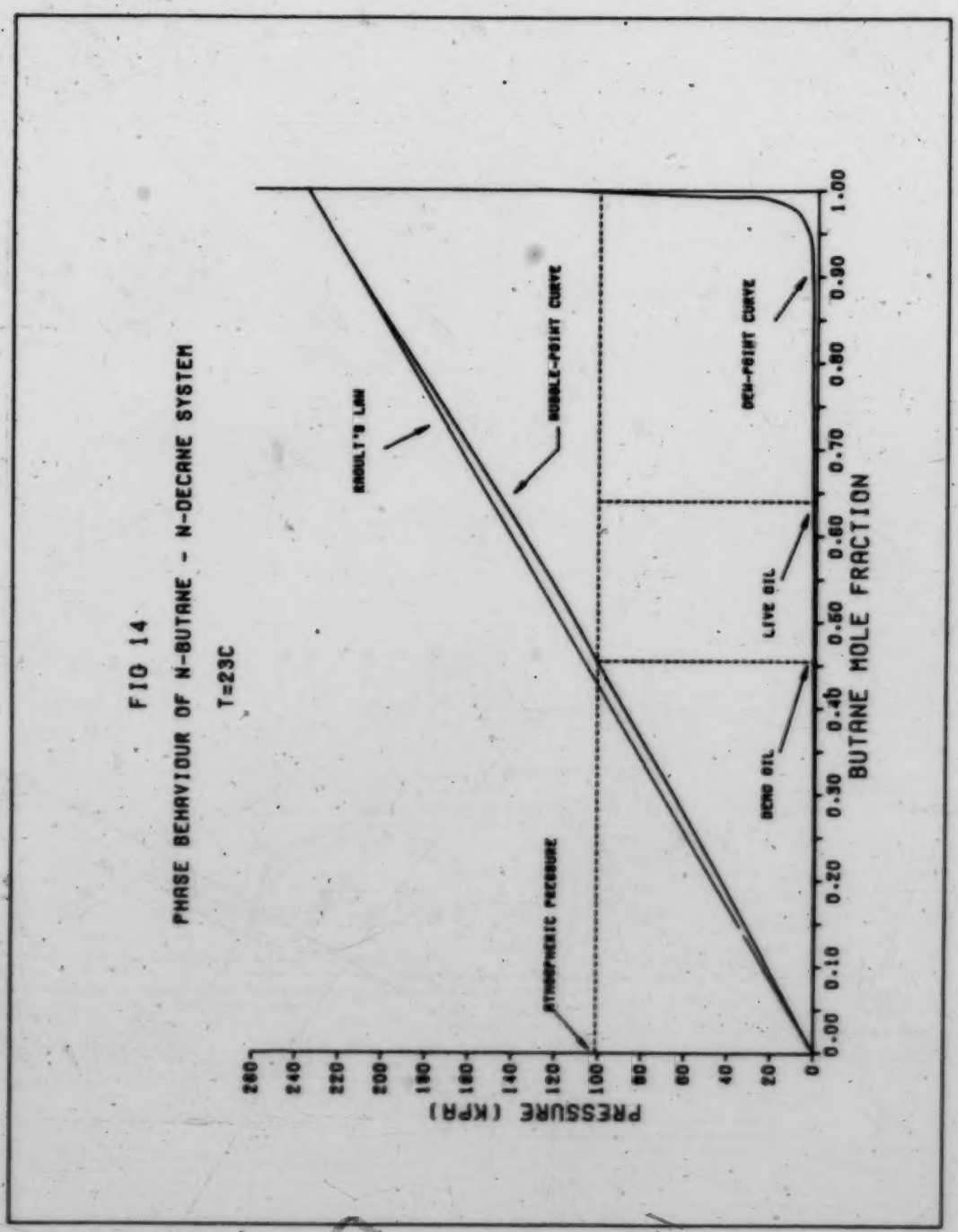

FIG 14

PHASE BEHAVIOUR OF N-BUTANE - N-DECANE SYSTEM

T=23C

had the same composition to that prior to breakthrough. This assumption was not very restrictive as the liquid volume produced after breakthrough was small compared to the total liquid volume ultimately recovered. A more accurate material balance would have required a knowledge of the composition of the liquid produced after breakthrough. Furthermore, as long as the same calculation procedure is utilized, a comparison of results obtained from different tests is possible. A verification was made by comparing the density of a separator liquid of a flashed live oil sample to atmospheric conditions and the average density of the produced liquid after a test. The values obtained agreed within 1%:

Oil density as calculated from published phase and volumetric behaviour of n-butane - n-decane system(20) :

0.687 gm/cc

Oil density as measured by flashing a live oil sample to atmospheric conditions :

0.691 gm/cc

Average oil density of total liquid produced (average over all displacement tests) :

0.695 gm/cc

The higher density for the liquid produced after a test is to be expected. Due to the stripping action of the displacing phase (methane), the oil produced after breakthrough will have a higher n-decane content, thus will be denser than the liquid produced prior to breakthrough.

6. Results and Discussion

6.1 Line of Investigation.

Based upon the literature survey, there does not appear to be universal agreement on the effects of various parameters on the results of a slim-tube miscible test. As a result, the effect of two parameters, characterizing the slim-tube displacement, were investigated, namely:

a) length of the system

b) rate of injection.

During the conduct of an experiment all other conditions were kept constant. The fluids were selected in order that the phase behaviour of the hc-system studied, could be represented rigorously on a ternary diagram. The three-component system chosen was the methane - n-butane - n-decane system, the phase behaviour of which has already been investigated(22,23,24). The oil displaced was composed of n-butane and n-decane with a composition fixed to 64 mole% n-butane and 36 mole% n-decane; this composition was chosen in order to operate at pressures below the specifications of the slim-tube apparatus (Pmaximum = 28,000 Kpa). The displacing fluid was methane. For such an idealized system, C1 represents the light ends, C4 the intermediates, and C10 the heavy ends.

The objective was to analyse the effect on recovery of length and injection rate at three different pressures and constant temperature. These pressures corresponded to the

immiscible case, the near MMP case, and the multiple-contact miscible case. The phase behaviour of the hc-system corresponding to each of these operating conditions is shown on Figure 15 and a summary of the operating variables is presented in Table 3.

6.2 Discussion of Results.

As a general observation, the displacements at a pressure of 24119 Kpa were all miscible, while the displacements at the other operating pressures were all judged immiscible. The displacement at a pressure of 20673 Kpa was very near miscibility for the longest system length considered (18.3m), based on the visual observation of the effluent in the sight glass.

6.2.1 Effect of Length and Injection Rate on Recovery.

6.2.1.1 Effect of Length.

The observed recoveries at 1.2 pore volume throughput, as a function of pressure, are illustrated in Figure 16. Before analysing this figure, it should be mentioned that a deviation of approximately 1% in the recovery values is to be expected, based upon a duplicate experiment of run No 3. A study of Figure 16 shows that an increase in length was translated into an upward shift of the recovery versus pressure relationship by as much as 10%. It may be observed that the total recovery (Rt) increases as length increases

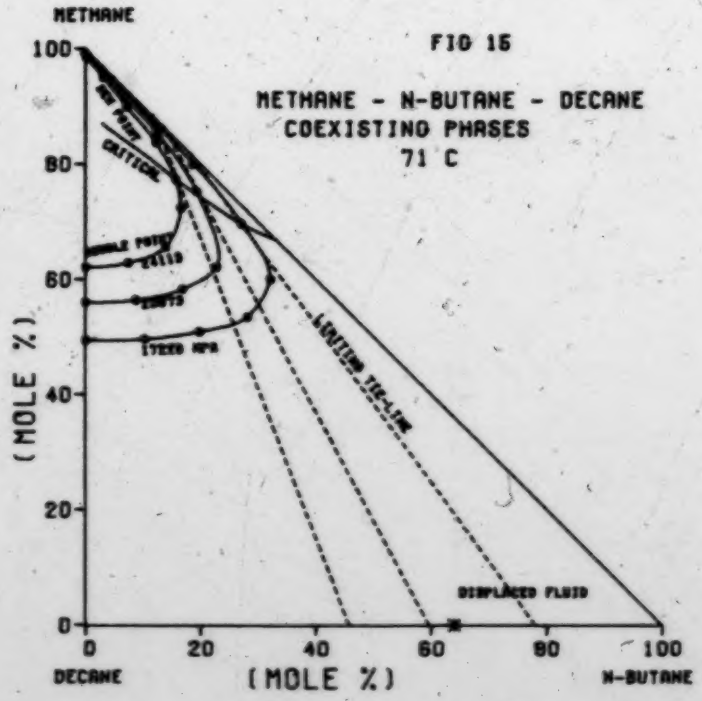

FIG 15

METHANE - N-BUTANE - DECANE
COEXISTING PHASES
71 C

Table 3

Summary of Operating Variables

Run No	Tube length (m)	Injection rate (V) (m/day)	Operating pressure (kpa)
01	06.1	20.7	17228
02	06.1	20.7	20673
03	06.1	20.7	24119
04	06.1	41.5	17228
05	06.1	41.5	20673
06	06.1	41.5	24119
07	06.1	84.8	17228
08	06.1	84.8	20673
09	06.1	84.8	24119
10	12.2	20.7	17228
11	12.2	20.7	20673
12	12.2	20.7	24119
13	12.2	41.5	17228
14	12.2	41.5	20673
15	12.2	41.5	24119
16	12.2	84.8	17228
17	12.2	84.8	20673
18	12.2	84.8	24119
19	18.3	41.5	17228
20	18.3	41.5	20673
21	18.3	41.5	24119
22	18.3	84.8	17228
23	18.3	84.8	20673
24	18.3	84.8	24119

FIG 16

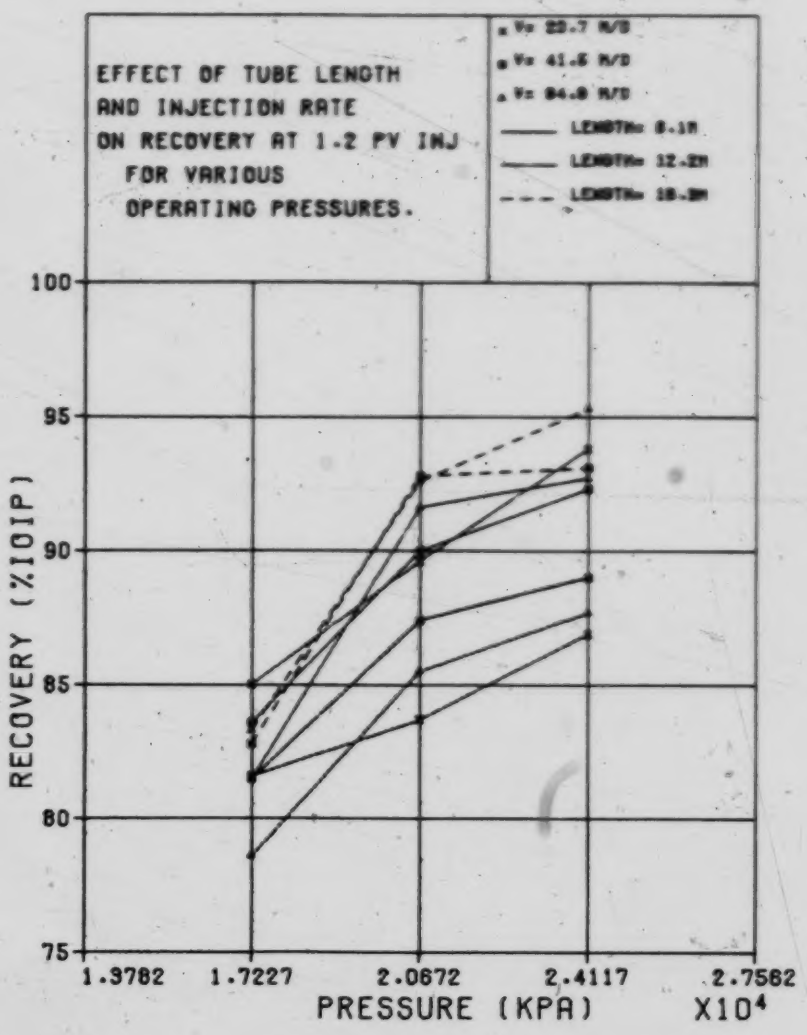
EFFECT OF TUBE LENGTH
AND INJECTION RATE
ON RECOVERY AT 1.2 PV INJ
FOR VARIOUS
OPERATING PRESSURES.
RECOVERY (%IOIP)
100
95
90
85
80
75
1.3782
1.7227
2.0672
2.4117
2.7582
PRESSURE (KPA)
X10⁴

for any injection rate. Also the rate of increase in Rt decreases as the length increases.

Generally, a vapourizing gas drive will start off as an immiscible displacement. Miscibility, if possible, is achieved through multiple contacts between the concurrently flowing phases, which implies that the gas at the front has to contact enough virgin oil, or travel a minimum length before miscibility is achieved. Also, the displacement of one fluid by another, and the mass transfer between the phases in contact occur simultaneously; thus, the phases present in a section of the porous medium are never rigorously in thermodynamic equilibrium, nor rigorously homogeneous. As thermodynamic equilibrium is more difficult to reach, the minimum length necessary for miscibility to be achieved will increase. Once miscibility is reached, the recovery is virtually 100% efficient except for some condensation behind the front, due to convective mixing in the gas phase. Also, the fingering of the gas and the consequent loss of miscibility will decrease the overall recovery because the gas will have to contact a certain amount of virgin oil before miscibility is reestablished. Hence, the reformation of the miscible front takes place at the cost of some residual oil left behind.

As noted by Rathmell(25), displacement in laboratory cores at a rate above a critical fingering

rate, may require substantial travel distances before full miscibility is achieved.

Let Rim, be the recovery obtained while traveling the length Li (immiscible portion) at a particular injection rate,

and Rm, be the recovery while traveling the length Lm (miscible portion) at the same injection rate.

The total recovery may be found by:

$$Rt = \frac{Rim \cdot Li + Rm \cdot Lm}{Lt} \qquad (21)$$

where

$$Lt = Li + Lm \qquad (22)$$

or

$$Rt = Rim\left(\frac{Li}{Lt}\right) + Rm\left(\frac{Lm}{Lt}\right) \qquad (23)$$

Assuming that the length Li is independent of the overall length of the system, the above formula (23) suggests that Rt will approach Rm, when Li/Lt is small, or when Lt is very large. Hence, the recovery (at 1 or 1.2 PVinj) will be characteristic of the multiple-contact miscible displacement only if the system length is long enough.

6.2.1.2 Effect of Injection rate.

The effect of injection rate is less obvious as no clear trend may be seen on Figure 16. However, it may be noted that increasing the system length tends to decrease the amount of scattering, especially in the

immiscible region. This lack of trend suggests that the displacement may be experiencing some instability at the rates considered. The same behaviour was observed by P. Deffrene *et al.*(2) for horizontal displacements. It appears that increasing the length has a stabilizing effect on the displacement which becomes almost rate independent. Another noticeable fact, is that for the cases where the displacements were conducted at the lowest injection rate, the curves show no clear break in slope, or in fact seem to break in the wrong direction.

However, for all cases, increasing the injection rate results in a break in slope which is more pronounced, and more clearly defined as the length is increased. This implies that increasing the rate decreases the recovery in the immiscible region, while it tends to level off the recovery in the miscible region for any length considered. It then permits the establishment of a better differentiation between multiple-contact miscible and immiscible displacements.

If one considers the case under the following operating conditions of 20673 Kpa pressure, 18.3m of length and 84.8m/d superficial velocity, the displacement was very near miscible, as judged by the visual observation through the sight glass. Although, only three operating pressures were considered for all the displacements, the above observation suggests that the MMP is very close to 20673 Kpa for the hc-system and

temperature considered. However, this value is somewhat higher than the estimated MMP of 19743 kpa, using the ternary diagram method. This value was obtained by correlating pressure versus the n-butane mole% in the n-butane - n-decane mixture corresponding to the intersection of the respective limiting tie-line with the abscissa (see Figure 15). The correlation is shown on Figure 17. Because of the fact that the displacement experienced instability, the above conservative observation was not unexpected. Therefore, from a thermodynamic stand-point, conventional slim-tube tests probably yield a conservative estimate of the MMP.

6.2.2 Effect of Length and Injection Rate on Concentration Profile.

To characterize the concentration profile, the butane concentration of the effluent gas was correlated with pore volumes injected. Before breakthrough, the gas evolving from the liquid phase at atmospheric conditions was only composed of butane. At breakthrough, the gas was mainly composed of butane and methane. The first appearance of methane can be easily picked up by the gas chromatograph.

6.2.2.1 Effect of Length.

For the multiple-contact miscible cases (Figures 18-20) and for the near miscibility cases (Figures 21-23), it can be observed that, independent of the injection rate considered, the concentration profile

FIG 17

CORRELATION OF MMP VS MOLE% BUTANE

IN BUTANE-DECANE MIXTURE (T=71C)

DISPLACING FLUID: METHANE

DISPLACED FLUID : BUTANE-DECANE MIXTURE

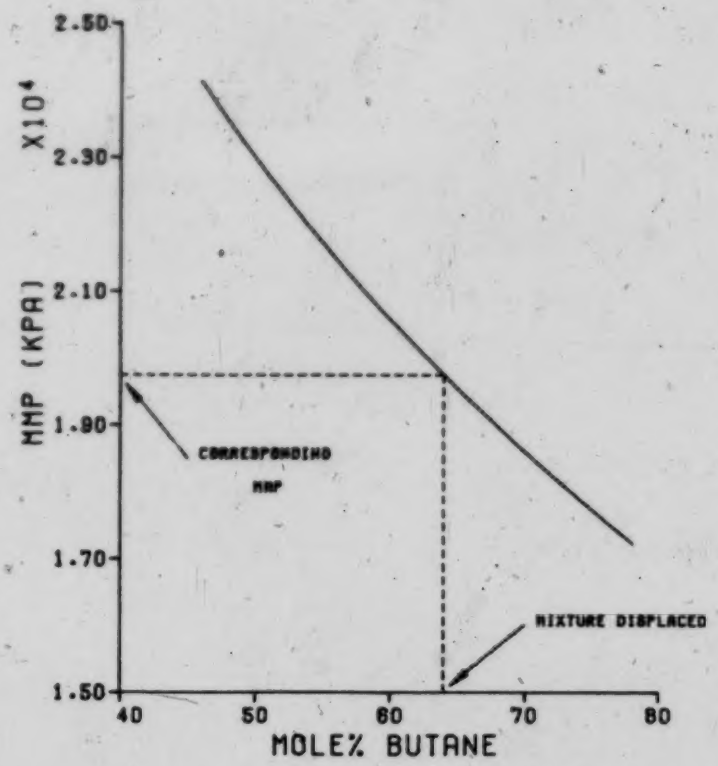

FIG 18

MISCIBLE CASE:

Effect of Tube Length and Injection Rate on Concentration Profile.

Operating Conditions:
*P = 24,118. kPa
*T = 71°C

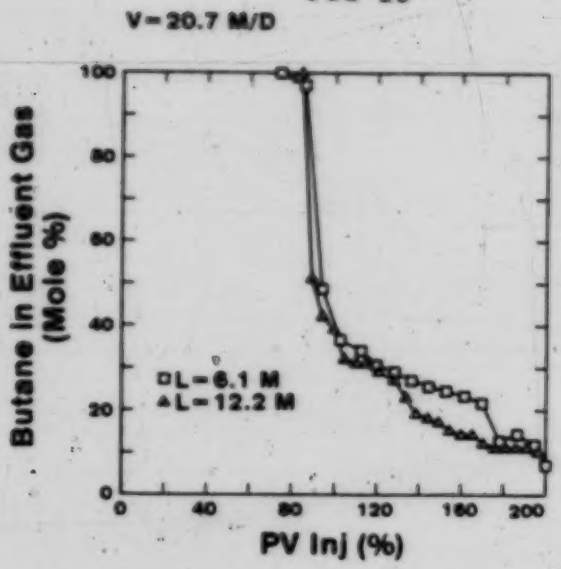

FIG 19

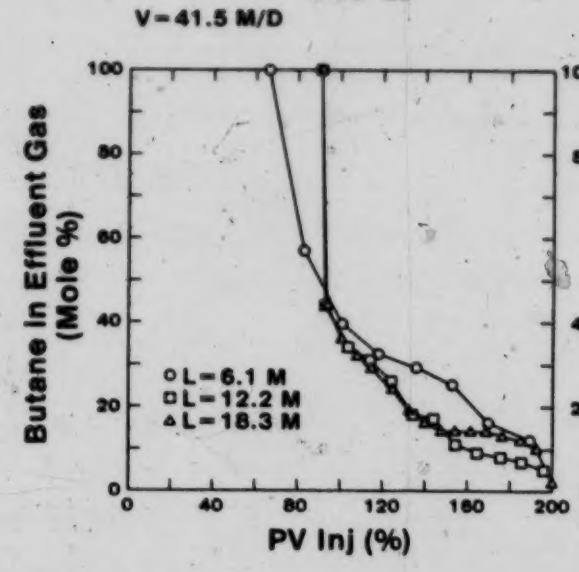

FIG 20

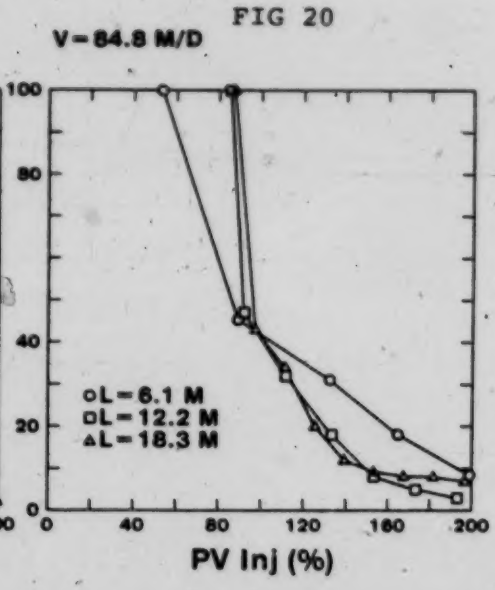

FIG 21

NEAR-MISCIBLE CASE:

Effect of Tube Length and Injection Rate on Concentration Profile.

Operating Conditions:
*P = 20,673. kPa
*T = 71°C

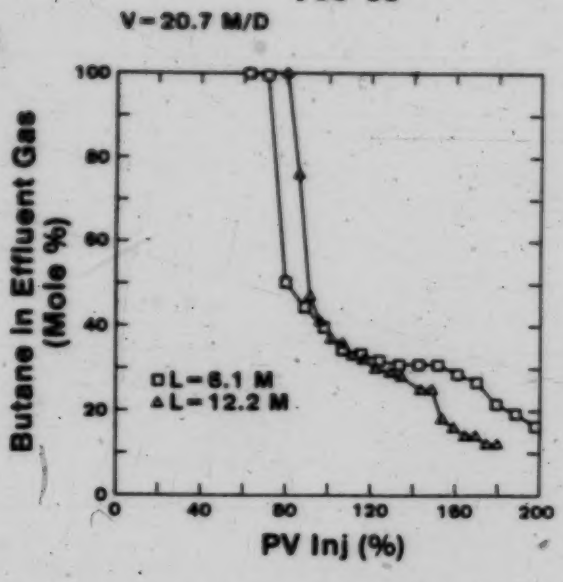

FIG 22

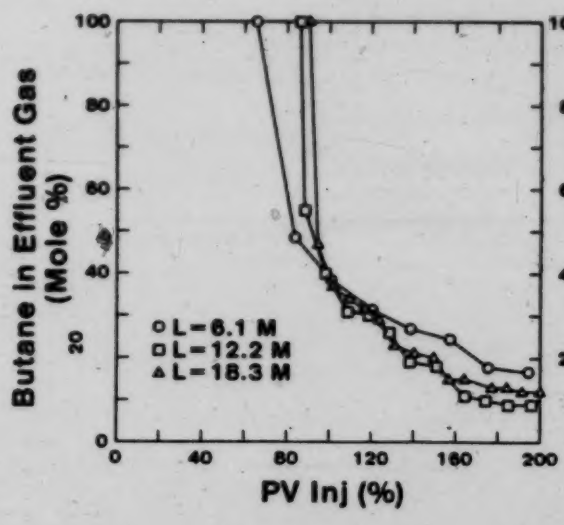

FIG 23

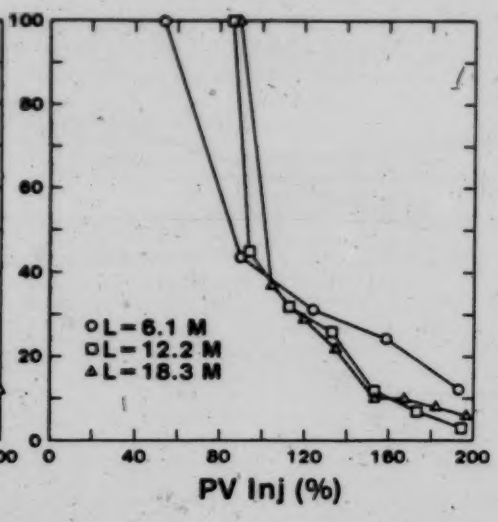

becomes sharper as the length increases. This signifies a better macroscopic sweep efficiency for the displacement as the length increases.

Also, the concentration profile tends to stabilize after a certain length is exceeded (12.2m), which agrees with the previous findings that the scattering of the points in the recovery curves decreases as length increases. As the injection rate is increased, the difference between the concentration profiles for the 6.1m tube as compared to the 12.2 and 18.3m tubes becomes more and more pronounced. It may also be observed that there is an earlier breakthrough for the 6.1m tube test. The gas breakthrough for the other two lengths investigated seems to stabilize near 90% pore volume injection.

For the immiscible cases (Figures 24-26), the length plays a lesser role and the concentration profiles seem to more or less coincide. However, there is still an earlier breakthrough of the displacing phase for the shortest length which is more noticeable as the rate increases. Also, a zone of higher butane concentration, corresponding to the plateau on the concentration profile, is more characteristic of the immiscible case as compared to the multiple-contact miscible and near-miscible cases. This again agrees with the earlier findings, that increasing the length favours potentially miscible displacements, and plays a lesser

IMMISCIBLE CASE:

Effect of Tube Length and Injection Rate on Concentration Profile.

Operating Conditions:
- P = 17,228 kPa
- T = 71°C

FIG 24

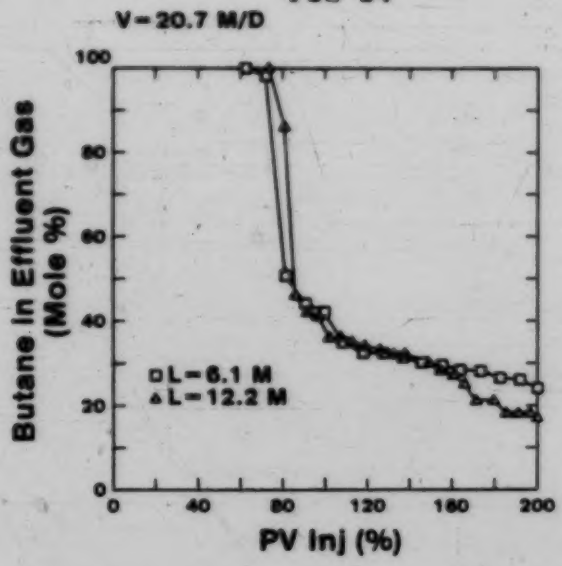

FIG 25

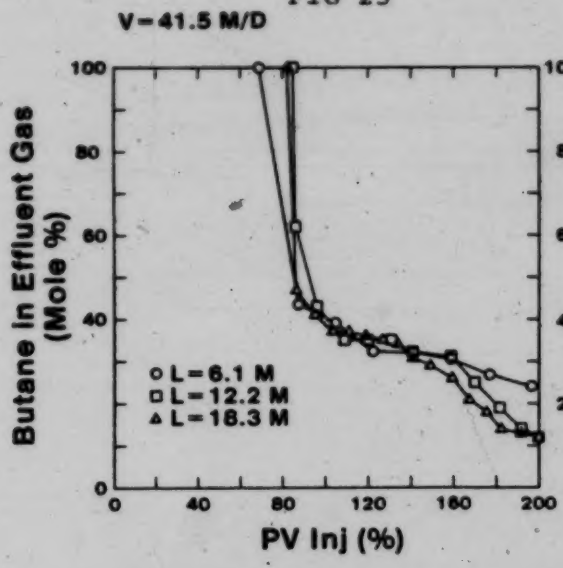

FIG 26

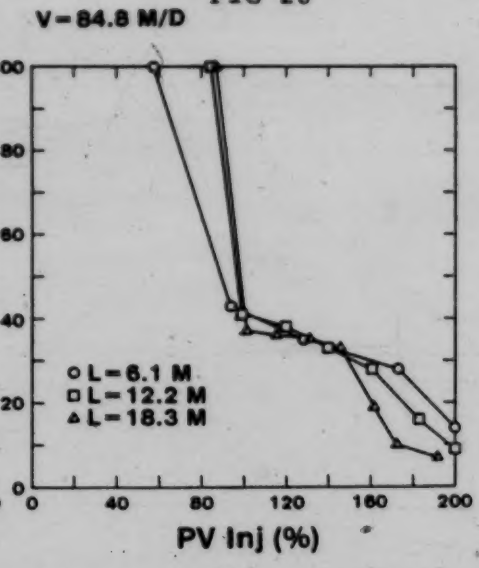

role for immiscible displacements. Hence, increasing the length permits the establishment of a better differentiation between immiscible and miscible displacements, and results in a more reliable value of the MMP.

Alonso *et al.*(24) and Rutherford(10) noted that multiple-contact miscible displacements in vertical cores, behave similarly to a first-contact miscible process with an S-shaped (no plateau) sharp concentration profile. For an immiscible displacement a distinctive plateau appeared in the concentration profile. For the multiple-contact miscible cases, in vertical cores, this behaviour was to be expected as high permeability and very low gas-oil capillary pressure in the diphasic zone behind the miscible front, allowed gravity forces to control the displacement and limit the length of the transition zone.

However, when dealing with a horizontal system, the gravity plays an adverse role by increasing the length of the transition zone. This effect is further increased when supercritical flow prevails. This is why the sharpness of the profile is less clearly defined and tends to level off to some low butane concentration, instead of becoming zero.

6.2.2.2 Effect of Injection Rate.

As previously mentioned, the higher the injection rate, the better is the segregation of the profiles

observed for the 6.1m tube test as compared to the 12.2 and 18.3m tubes. The greater the length, the less dependent is the concentration profile on injection rate. In other words:

For short length tubes: displacement is very much rate dependent.

For long length tubes: displacement is less rate dependent.

6.2.3 Analysis of the Extreme Cases.

To further emphasize the results of this investigation, one should analyse the extreme cases, (Figures 27-30):

Case (A) : shortest length, lowest injection rate

Case (B) : longest length, highest injection rate.

An examination of these two extreme cases resulted in the following observations:

a) While the recovery curve of case (B) shows a clear break in slope, case (A) shows almost no change in slope (see Figure 27).

b) The break in slope of case (B) which occurs approximately at a value of 20673 Kpa, agrees with the visual observation in the sight glass of the displacement being near miscibility conditions.

c) For case (B), multiple-contact miscible displacements are characterized by a relatively sharp concentration profile, while a distinctive plateau appears for the immiscible displacement. On the other hand, case (A)

FIG 27

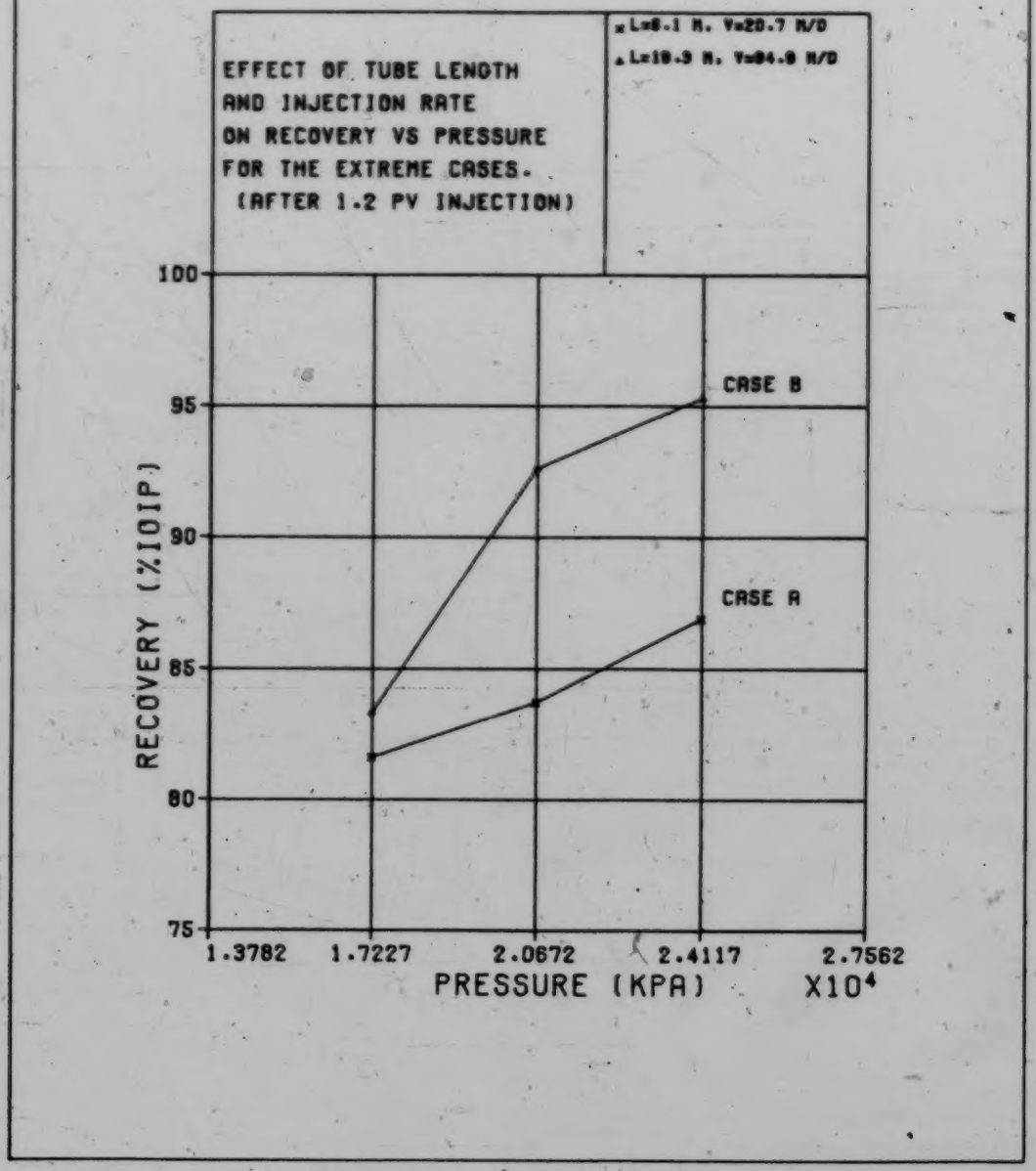
EFFECT OF TUBE LENGTH
AND INJECTION RATE
ON RECOVERY VS PRESSURE
FOR THE EXTREME CASES.
(AFTER 1.2 PV INJECTION)
x L=6.1 M. V=20.7 M/D
▲ L=18.3 M. V=84.8 M/D
CASE B
CASE A
RECOVERY (%IOIP)
100
95
90
85
80
75
1.3782
1.7227
2.0672
2.4117
2.7562
PRESSURE (KPA) X10⁴

FIG 28

EXTREME CASES:

Effect of Tube Length and Injection Rate on Concentration Profile for Extreme Cases A & B, at Various Pressures.

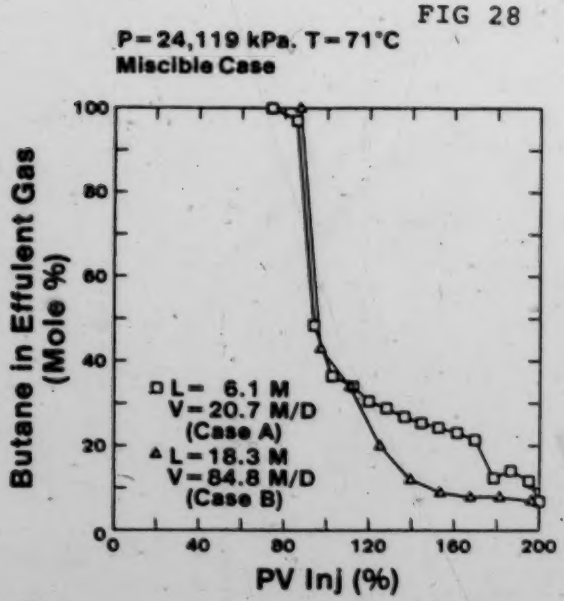

FIG 29

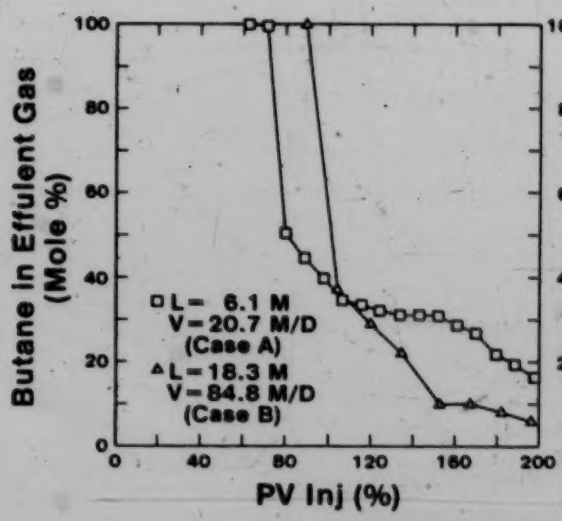

FIG 30

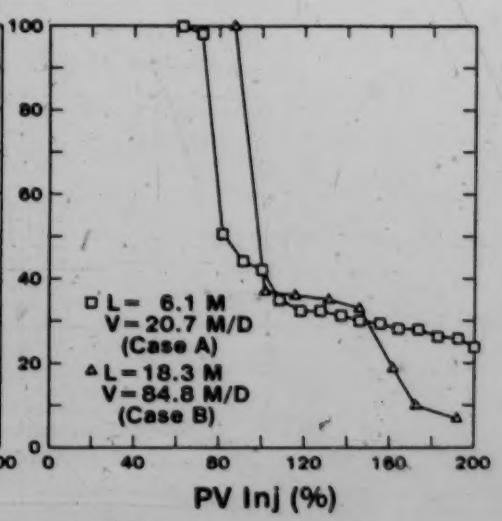

does not show such a clear distinction (see Figures 28-30).

d) The time necessary to perform the experiment was shorter for case (B) than case (A).

7. CONCLUSIONS

Based upon this limited number of experiments, the hc-system studied, and the fact that only one tube diameter was used, it may be concluded that:

a) Because the recovery has been found to be affected by the system length and injection rate, in order to determine the MMP, one should not use as the only criterion that the recovery be greater than some fixed value at some pore volume injected.

b) The MMP depended to a great extent on the length of the system, and to a lesser extent on the injection rate provided the system length was sufficiently long.

c) In general, the longer the system, the smaller the relative length immiscibly displaced, and the better the estimation of the MMP. It appears that a minimum of 12.2m of length was required.

d) A better differentiation between immiscible and multiple-contact miscible vapourizing gas drives, as conducted in flat coil slim-tubes, is obtained at high injection rates.

e) The MMP was found to be conservative when compared to the estimated value obtained by the ternary diagram method for

the hc-system investigated.

f) Determination of the MMP based upon the visual observation through the sight glass was not sufficient, because what was observed was found to be a function of length and injection rate.

7.1 RECOMMENDATIONS

If the MMP is to be determined experimentally using a flat slim-tube coil, the following should be considered:

a) System length: The length should be as long as possible, so that the minimum length of immiscible displacement necessary for miscibility to be dynamically created, will not mask the overall effect of the multiple-contact miscible displacement.

b) Tube diameter: The inner diameter should be small in order to reduce the effect of gravity and fingering. However, any reduction of the ID should be accompanied with a reduction of the particle diameter, so that the ratio of particle diameter to tube diameter is less than 0.01 minimizing any wall effects(27).

c) Injection rate: The rate of injection is not critical, so long as the length of the system is sufficiently long. For a long system, the injection rate

would have to be increased in order to conduct the experiment in a relatively short time. Moreover, a moderately high injection rate is preferable in order to obtain a better differentiation between immiscible and multiple-contact miscible displacements.

NOMENCLATURE

C1-N2 = methane, nitrogen

C2-C6 = ethane to hexane

C7+ = heptane plus

C*= wettability number, dimensionless

D = core diameter, m

g = gravitational acceleration, m/sec^2

ID = inside diameter, m

IOIP = initial oil in place

Isc = dimensionless number for cylindrical system

K = intrinsic permeability, m^2

K1 = maximum effective permeability to fluid 1, m^2

K2 = maximum effective permeability to fluid 2, m^2

Kgor = permeability to gas at irreducible oil saturation, m^2

Kogr = permeability to oil at irreducible gas saturation, m^2

Kr1 = maximum relative permeability to fluid 1

Kr2 = maximum relative permeability to fluid 2

M = mobilty ratio

MMP = minimum miscibility pressure, Kpa

Ng = gravity number, dimensionless

PVinj = pore volume injected, %

So = oil saturation, fraction

Sor = irreducible oil saturation, fraction

V = superficial velocity, m/sec

Vc = critical velocity, m/sec

Vc-immiscible = critical velocity for immiscible displacement, m/sec

Vc-miscible = critical velocity for miscible displacement, m/sec

Vd = Darcy velocity, m/sec

ρ_1 = density of fluid 1, Kg/m^3

ρ_2 = density of fluid 2, Kg/m^3

ρ_g = gas density, Kg/m^3

ρ_o = oil density, Kg/m^3

$\nabla\rho$ = displaced fluid - displacing fluid density difference, Kg/m^3

μ_1 = viscosity of fluid 1, pa.sec

μ_2 = viscosity of fluid 2, pa.sec

μ_g = gas viscosity, pa.sec

μ_o = oil viscosity, pa.sec

θ = angle core makes with the horizontal, radians

α = angle core makes with the vertical, radians

REFERENCES

1. F.M. Orr, M.K. Silva, C.L. Lien, M.T. Pelletier, "Laboratory Experiments to Evaluate Field Prospects for CO2 Flooding" JPT,(Apr 1982).

2. P. Deffrene, C. Marle, J. Pacsirszky, M. Jeantet, "La Détermination des Pressions de Miscibilité", Revue IFP16,N6,(June 1961),678.

3. C.A. Hutchinson, P.H. Braun, "Phase Behaviour of Miscible Displacement in Oil Recovery", A.I.CH.E. Journal,(March 1961),Vol7,N1,64.

4. R.L. Slobod, H.A. Koch, "High-Pressure Gas Injection - Mechanism of Recovery Increase", OIL and GAS J.,(1953)51,84.

5. S.E. Buckley, M.C. Leverett,Trans. AIME 146,107(1942).

6. A. Giraud, R. Thomere, "Miscibilité Dynamique.Contribution a L' étude des Zones de Melanges", Revue IFP,(May 1968),619.

7. P.M. Sigmund, "Prediction of Molecular Diffusion at Reservoir Conditions. Part II- Estimating the Effects of Molecular Diffusion and Convective Mixing in Multicomponent Systms", JCPT,(July-September 1976),53.

8. Engineering Data Book, Natural Gasoline Supply Men's Association(1957).

9. A.L. Benham, W.E. Dowden, W.J. Kunzman, "Miscible Fluid Displacement - Prediction of Miscibility", Trans.,AIME(1959)216,388.

10. W.M Rutherford, "Miscibility Relationships in the Displacement of Oil by Light Hydrocarbons", Trans.,AIME(1962)222,II-340.

11. W.F. Yellig, R.S. Metcalfe, "Determination and Prediction of CO2 Minimum Miscibility Pressures", JPT,(Jan 1980),160.

12. L.W. Holm, V.A. Josendal, "Mechanism of Oil Displacement by Carbon Dioxide", JPT,(Dec 1974),1427.

13. F.E. Crane, H.A. Kendall and G.H.F. Gardner, "Some Experiments on the Flow of Miscible Fluids of Unequal Density Through Porous Media", SPE.J., (Dec 1963), 277.

14. J.M. Dumoré, "Stability Considerations in Downward

Miscible Displacements", SPE.J.,(Dec 1964),356.

15. C.M. Marle,"Multiphase Flow in Porous Media", IFP Publications, Editions Technip(1981).

16. R.G. Hawthorne, "Two-phase Flow in Two-dimensional Systems - Effects of Rate, Viscosity and Density on Fluid Displacement in Porous Media", Trans.AIME,219,(1960),81.

17. E.J. Peters and D.L. Flock, "The Onset of Instability During Two-phase Immiscible Displacement in Porous Media", SPE.J., (Apr 1981), 249.

18. Fred I. Stalkup Jr., "Status of Miscible Displacement", JPT, (Apr 1983), 815.

19. R.J. Blackwell, J.R. Rayne, W.M. Terry, "Factors Influencing the Efficiency of Miscible Displacements", Trans.,AIME(1959)216,1.

20. C.Van Der Poel, "Effect of Lateral Diffusivity on Miscible Displacement in Horizontal Reservoirs", SPE.J,(Dec 1962),317.

21. D.L. Katz, D. Cornell, R. Kobayashi, J.R. Elenbaas and C.F. Weinaug, "Handbook of Natural Gas Engineering", Mc Graw-Hill Book Company, INC. New York,1959.

22. R.H. Olds, B.H. Sage, W.N. Lacey, "Partial Volumetric Behaviour in the n-Butane - Decane System", Fundamental Research on Occurrence and Recovery of Petroleum, API(1948-1949),25-43.

23. B.H. Sage, W.N. Lacey, "Some Properties of the Lighter Hydrocarbons, Hydrogen Sulfide, and Carbon Dioxide", Monograph on API Research Project 37, API(9155),229-241.

24. B.H. Sage, W.N. Lacey, "Thermodynamic Properties of the Lighter Paraffin Hydrocarbons and Nitrogen", Monograph on API Research Project 37, API(1950),203-219.

25. J.J. Rathmell, F.I. Stalkup, R.C. Hassinger, "A Laboratory Investigation of Miscible Displacement by Carbon Dioxide", 46th Annual Fall Meeting of SPE of AIME,New Orleans,La., Oct. 3-6, 1971.SPE No 3483.

26. M. Alonso, Y. Morineau, P. Simandoux, A.D. Bradshaw and D.W.Bennion, "A Laboratory Investigation of the Enriched Gas Displacement Process in Vertical Model", JCPT,(Jan-March 1973),47.

27. T.K. Perkins, D.C. Johnston, "A Review of Diffusion and Dispersion in Porous Media", SPE.J.,(1963)3,70.

28. G.E. Archie, "The Electrical Resistivity Log as an Aid in Determining Some Reservoir Characteristics", Trans.AIME,v.146,1942,54.

29. P.M. Sigmund, "Prediction of Molecular Diffusion at Reservoir Conditions. Part I - Measurement and Predictions of Binary Dense Gas Diffusion Coefficients", J.C.P.T,(April-June 1976),48.

30. J.O. Hirschfelder, C.F. Curtiss and R.B. Bird, "Molecular Theory of Gases and Liquids", John Wiley and Sons INC, New York, 1964.

31. L.I. Stiel and G. Thodos, "Lennard-Jones Force Constants Predicted From Critical Properties", J.Chem.Eng.Data,7,235(1962).

APPENDIX 1: Definition of Dispersion Coefficient in Porous Media

In order to differentiate diffusion in porous media from that in an open system (eg:capillary tube) we need to assess what characterizes a porous medium. A porous medium can be idealized by a bundle of interconnected tortuous flow channels and with a reduced area open to flow.

We will first consider molecular diffusion in porous media by drawing the analogy between Fick's law and Ohm's law. The convective mixing portion of the total dispersion will then be considered, and an effective dispersion coefficient will be defined.

1) Analogy Between Fick's law and Ohm's law.

Consider the case where two single-component miscible fluids of equal densities and molecular diffusivities are brought into contact in a linear system. The equation governing the diffusion is given by Fick's law:

$$\frac{dmi}{dt} = -Do\ A\ \frac{d\rho Ci}{dx}_{i=1,2} \qquad (24)$$

where,

dmi/dt = rate of mass transfer of component i

Do = molecular diffusivity

A = area open to diffusion

ρ = density of the diffusing fluid

Ci = mass fraction of component i in diffusing mixture

x = distance traveled by the diffusing component

t = time

Consider now the case of conduction in a linear system saturated for example with water. The equation governing conduction of electricity is given by Ohm's law:

$$\frac{dq}{dt} = -\frac{A}{Rw} \cdot \frac{dp}{dx} \qquad (25)$$

where,

dq/dt = intensity of the current

Rw = resistivity of water

A = area open to flow

P = potential

x = distance traveled by the charges

t = time

One may then make the following analogy:

	Fick's law		Ohm's law
rate of transfer:	dmi/dt	≡	dq/dt
area open to flow:	A	≡	A
rate of change of potential:	dC/dx	≡	dP/dx
conduction:	Do	≡	1/Rw

2) Molecular Diffusion in Porous Media.

In this section we will solve for the effective resistivity of a porous medium saturated with water. Using the analogy between Fick's law and Ohm's law, we will then obtain the effective molecular diffusivity in porous media.

Consider a porous medium of porosity, $\emptyset$, saturated with water. An idealized system may be characterized by a series of tortuous flow paths as illustrated in Figure 31.
A macroscopic average path length can be obtained, given by:

$$X' = \alpha X \quad \text{where, } \alpha \text{ is a tortuosity factor} \tag{26}$$

and the average area open to flow is given by:

$$A' = (\emptyset A X)/X' = \emptyset A/\alpha \tag{27}$$

Such a system is equivalent to a single straight flow path (see Figure 31). Writing Ohm's law for the equivalent system:

$$\frac{dq}{dt} = -\frac{A'}{Rw} \cdot \frac{dP}{dX'} \tag{28}$$

substituting for A' and X'

$$\frac{dq}{dt} = -\frac{\phi}{\alpha^2 Rw} \cdot \frac{dP}{dX} \tag{29}$$

The factor $\alpha^2/\emptyset$ is termed the formation resistivity factor, F, and can be determined by Archie's equation for sands(28):

$$F = 0.62/\emptyset^2 \tag{30}$$

Making the analogy between Fick's law and Ohm's law, the

FIG 31

EQUIVALENT SYSTEM OF AN IDEAL
POROUS MEDIUM SATURATED WITH WATER
OF RESISTIVITY RW

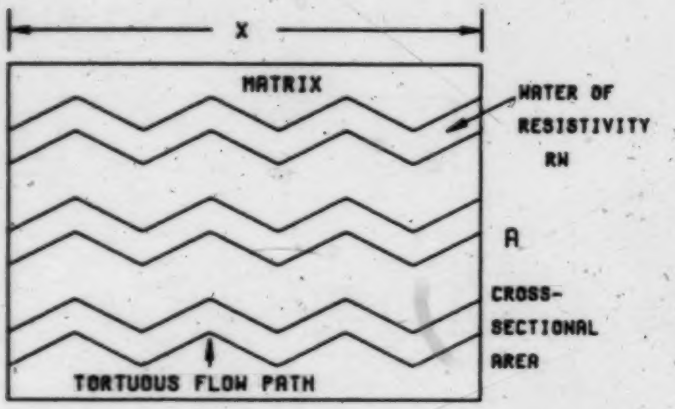

EQUIVALENT TO

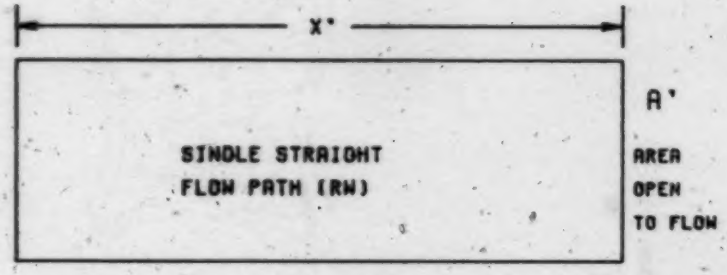

$$A' = \frac{\phi}{\alpha} A \; ; \; X' = \alpha X$$

following equivalence statements can be formulated:

In the absence of porous medium:	Do	≡	1/Rw
For a porous medium:	D	≡	1/FRw

hence, $$\frac{Do}{D} = \frac{1/Rw}{1/FRw}$$

The effective molecular diffusion coefficient in porous media[4] is then given by:

$$D = \frac{Do}{F} \qquad (31)$$

3) Convective Mixing in Porous Media.

It has been shown that a porous medium can be characterized by a bundle of interconnected flow channels. However, dissimilar flow channels will result in different average interstitial velocities. Consequently, particles of fluid will travel at different speeds in different flow channels. If these particles have different compositions, an additional mixing will occur at the intersection of these

---

[4]Note that in this definition of the effective molecular diffusion coefficient, we are considering the total cross-sectional area instead of the area open to flow.

channels. This additional mixing has been termed convective mixing. An empirical experimental relationship describing this phenomenon has been found(27) and is given by:

$$Kconv = \sigma \cdot Vd \cdot dp \qquad (32)$$

where,

Kconv = effective convective diffusion coefficient

Vd = average darcy velocity

dp = average particle diameter

σ = factor accounting for the inhomogeneity of the medium, the ratio of the particle diameter to the lateral dimensions, the particle size distribution and the particle shape.

4) Effective Dispersion Coefficient in Porous Media.

The effective dispersion coefficient in porous media is found by simply superimposing the effects of molecular diffusion and convective mixing, and is given by:

$$K = \frac{Do}{F} + \sigma \cdot Vd \cdot dp \qquad (33)$$

Where in cgs units we have:

K = effective dispersion coefficient, cm^2/sec

Do= molecular diffusion coefficient, cm^2/sec

F = formation resistivity factor

Vd = average darcy velocity, cm/sec

dp = average particle diameter, cm.

Note again, that in this definition of the effective dispersion coefficient, the total cross-sectional area is used instead of the area open to flow. The equation governing dispersion in porous media is then given by:

$$\frac{dm}{dt} = - K A \frac{d\rho c}{dx} \qquad (34)$$

where A is the total cross-sectional area.

APPENDIX 2: Effect of Molecular Diffusion and Convective Mixing in Multicomponent Systems

The purpose of this discussion is to assess the effect of components diffusing at different rates in a miscible displacement. In order to examine this effect, a comparison will be made of the composition profiles obtained by considering different diffusion coefficients for different diffusing species, as opposed to a common diffusion coefficient for all components. The differential equation describing the composition change of each component in a diffusing mixture as a function of time and position will first be considered. For the sake of simplicity, a one-dimensional first-contact miscible displacement in an infinite porous medium will be considered, for which analytical solutions to the differential equation are available.

A method for estimating diffusion coefficients in a multicomponent diffusing mixture will be discussed. This method follows the procedure outlined by Sigmund(7,29). An example will be presented in order to illustrate the above stated effect.

1) Continuity Equation.

Consider a first-contact miscible displacement in a one-dimensional open system (porosity=1). Assuming that no change in volume occurs upon mixing, the differential equation describing the composition change of each component in a diffusing mixture of n+1 components with respect to time and space is given by:

$$-\frac{\partial}{\partial x}\left(Ci\ Vb - \sum_{k=1}^{n} Dik \frac{\partial Ck}{\partial x}\right) = \frac{\partial Ci}{\partial t}\quad i=1,n \tag{35}$$

where,

Ci = molar concentration, gmole/cc

Dii = main diffusion coefficient, cm^2/sec

$D_{i\neq k}^{ik}$ = is a measure of the coupling or interaction that takes place between the n+1 diffusing species, cm^2/sec

Vb = bulk flow velocity, cm/sec

x = space variable, cm

t = time variable, sec

The effect of coupling can be conveniently taken into account by defining an effective diffusion coefficient, Dim, for each component i and Equation (35) can be written as:

$$\frac{\partial}{\partial x}\left(Dim \frac{\partial Ci}{\partial x} - Vb\ Ci = \frac{\partial Ci}{\partial t}\right)_{i=1,n} \tag{36}$$

If one assumes a constant average density for the diffusing mixture, $\bar{\rho}$, and that Dim is independent of concentration and

is determined at the average density $\bar{\rho}$, for constant bulk flow velocity Equation (36) is further simplified to:

$$Dim \frac{\partial^2 Yi}{dx^2} - Vb \frac{\partial Yi}{dx} = \frac{\partial Yi}{\partial t} \qquad i=1,n \qquad (37)$$

where, Yi = mole fraction of component i = $Ci/\bar{\rho}$

Assuming flow in a porous medium where convective mixing is not negligible, the effective diffusion coefficient of component i becomes (refer to Appendix 1):

$$Kim = \frac{Dim}{F} + \sigma \cdot Vd \cdot dp \qquad (38)$$

where,

F = formation resistivity factor

$\emptyset$ = porosity

Vd = darcy velocity, cm/sec

dp = average particle diameter, cm

Dim = molecular diffusion coefficient of component i, cm^2/sec

Kim = dispersion coefficient of component i, cm^2/sec

σ = factor accounting for the inhomogeneity of the medium the ratio of the particle diameter to the lateral dimensions, the particle size distribution and the particle shape.

Equation (37) becomes:

$$Kim \frac{\partial^2 Yi}{\partial x^2} - Vd \frac{\partial Yi}{\partial x} = \phi \frac{\partial Yi}{\partial t} \qquad (39)$$

or

$$K_{im} \frac{\partial^2 y_i}{\partial x^2} - V \frac{\partial y_i}{\partial x} = \frac{\partial y_i}{\partial t} \qquad (40)$$

where, $K'_{im} = K_{im}/\phi$

V = average interstitial velocity, cm/sec.

If one considers an infinite linear porous medium where a fluid of initial composition $Y_{i\bar{o}}$ displaces another of composition $Y_{i\hat{o}}$, the solution to Equation (40) is given by:

$$Y_{ie} = Y_{i\bar{o}} + \frac{1}{2} \operatorname{erfc}\left(\frac{XD}{2\sqrt{K_{im}\, t}}\right) \cdot (Y_{i\hat{o}} - Y_{i\bar{o}}) \qquad (41)$$

Where, XD = X - Vt = distance from initial interface, cm

In general $\sum_{i=1}^{n+1} Y_{ie} \neq 1.0$, since the components diffuse at different rates, and the results should be normalized using the relationship:

$$Y_i = \frac{Y_{ie}}{\sum_{i=1}^{n+1} Y_{ie}} \qquad (42)$$

2) Estimation of the Effective Molecular Diffusion Coefficient, Dim.

Suppose the displacement is conducted at some average operating condition of pressure and temperature. Let $\overline{Y_i}$ be the mole fraction of component i in the average diffusing mixture. $\overline{Y_i}$ is defined as:

$$\overline{Y_i} = \frac{Y_{i\bar{o}} + Y_{i\hat{o}}}{2} \qquad (43)$$

The average molar density of the diffusing mixture is given by:

$$\bar{\rho} = \sum_{i=1}^{n+1} \overline{Yi}\ \rho i \qquad (44)$$

Let ρc^{5} be the critical molar density of the system studied at the conditions of pressure P and temperature T. The reduced average molar density is defined by:

$$Pr = \frac{\bar{\rho}}{\rho c} \qquad (45)$$

From the generalized reduced density correlation for predicting dense fluid diffusion coefficients(7):

for every pair of components i,j , the mutual diffusion coefficient $\mathcal{D}ij$ can be calculated from the following expression:

$$\frac{\rho ij\ Dij}{\rho^{\circ}ij\ D^{\circ}ij} = a + bPr + cPr^2 + dPr^3 \qquad (46)$$

where,

ρij = average molar density of binary system (i,j) in the diffusing mixture = $(\rho i\ \overline{Yi} + \rho j\ \overline{Yj})/(\overline{Yi} + \overline{Yj})$

ρi = molar density of component i in i,j mixture of composition $\overline{Yi}/(\overline{Yi} + \overline{Yj})$, $\overline{Yj}/(\overline{Yi} + \overline{Yj})$

$\mathcal{D}ij$ = mutual diffusion coefficient of binary system (i,j) = ji

$\rho^{\circ}ij\mathcal{D}^{\circ}ij$ = is the zero pressure limit of the

---

[5] ρc is uniquely defined only if we consider a ternary system at constant pressure and temperature. In a complex hc-system, ρc is only an approximation based on the representation of the phase behaviour of the system on a pseudo-ternary diagram.

density-diffusivity product and is estimated from Chapman-Enskog dilute gas theory(30)

The constant a, b, c, and d take on the following values:

a = 0.99589

b = 0.096016

c = -0.22035

d = 0.032874

$\rho^*_{ij}D^*_{ij}$ can be estimated from the following formula:

$$\rho^*_{ij}\, D^*_{ij} = \frac{0.0018583\left(\frac{1}{Mi}+\frac{1}{Mi}\right)^{1/2}\cdot T^{1/2}}{\sigma_{ij}^2\,\Omega_{ij}\,R} \qquad (47)$$

where, Mi, Mj = molecular weight of components i and j, respectively

T = temperature, K°

R = universal gas constant

= 82.057 cc.atm/K°.mole

σ_{ij} = collision diameter for Lennard-Jones potential, A

Ω_{ij} = collision integral function.

σ_{ij} and Ω_{ij} can be estimated from Stiel and Thodos correlation(31):

$$\Omega_{ij} = \Omega^{(1,1)^*}(T^*_{ij}) \qquad (48)$$

$$T^*_{ij} = \frac{k}{\varepsilon_{ij}}T \qquad (49)$$

$$\sigma_{ij} = 0.1866\ p_{Vc}^{1/3}\,p_{Zc}^{0.4} \qquad (50)$$

$$\frac{\varepsilon_{ij}}{k} = 65.3\ p_{Tc}\ p_{Zc}^{3.4} \qquad (51)$$

where, $\frac{\varepsilon ij}{K}$ = energy parameter, K°

$\Omega^{(1,1)^*}$ = tabulated as a function of T^6

$_pTc$ = pseudo critical temperature of binary system i,j = $(\overline{Yi}\ Tci + \overline{Yj}\ Tcj)/(\overline{Yi} + \overline{Yj})$, K°

$_pPc$ = pseudo critical pressure of binary system i,j = $(\overline{Yi}\ Pci + \overline{Yj}\ Pcj)/(\overline{Yi} + \overline{Yj})$, atm

$_pVc$ = pseudo molar volume of binary system i,j = $(\overline{Yi}\ \overline{ci} + \overline{Yj}\ \overline{cj})/(\overline{Yi} + \overline{Yj})$, cc/gmole

$_pZc$ = pseudo compressibility of binary system i,j = $_pPc\ _pvc/R\ _pTc$

Finally, the effective diffusion coefficient Dim can be estimated from the Wilk effective diffusivity Equation(7) :

$$Dim = \frac{1 - \overline{Yi}}{\sum_{k=1\ k\neq i}^{n+1} \overline{Yk}/\mathcal{D}ik} \qquad (52)$$

---

[6] $\Omega^{(1,1)^*}$ are tabulated as a function of T^* in Table I-M, page 1126, of reference(30).

SAMPLE PROBLEM: First-contact Miscible Displacement of Methane-decane by Methane-butane

The following example illustrates the effect of components diffusing at different rates on the composition profile as opposed to a common diffusion coefficient for all components. A three-component hc-system will be considered, methane - n-butane - n-decane, whose phase behaviour can be represented rigorously on a ternary diagram at some fixed conditions of pressure and temperature. It will be assumed that the assumptions made for the calculation of the composition profiles using Equation (41) are applicable. The effective diffusion coefficient for each component will be estimated following the method previously outlined. In order to compare the two cases, the respective composition paths will be plotted on the ternary diagram. Calculation of the composition profile for the case where a common diffusion coefficient is assumed for all the diffusing species is not necessary since the corresponding composition path on the ternary diagram will be simply the straight line joining the points representing the displaced and displacing fluid compositions.

Assume that the following parameters and conditions apply:

a) Equation (41) applies, that is the composition profile of each component is given by:

$$Yie = \bar{Yio} + \frac{1}{2}\,\mathrm{erfc}\,\frac{XD}{2\sqrt{Kim\ t}} \cdot (\overset{+}{Yio} - \bar{Yio})_{i=1,3}$$

$$Yi\ (XD,t) = \frac{Yie}{\sum_{i=1}^{3} Yie}$$

b) V, the average interstitial velocity, is small enough for convective mixing to be neglected. (Molecular diffusion is controlling, V=0)

c) Average operating conditions: P = 13783 kpa, T = 71c

d) Porosity = Ø = 0.3

e) Formation resistivity factor is estimated from 'Archie's equation

f) Time = 1 year.

Initial Fluid Compositions

component	i	XD<0 Displacing fluid $\bar{Yio}$	XD>0 Displaced fluid $\overset{+}{Yio}$
CH4	1	0.520	0.200
C4H10	2	0.480	0.000
C10H22	3	0.000	0.800

1) Estimation of Effective Diffusion Coefficients, Dim.

a) Average density of diffusing mixture:

Average diffusing mixture composition:

$\overline{Y1} = 0.360$

$\overline{Y2} = 0.240$

$\overline{Y3} = 0.400$

and obtain:

$$\bar{\rho} = 0.00789 \text{ gmole/cc}$$

b) Density of critical mixture:

critical mixture composition:

$Y1c = 0.665$

$Y2c = 0.320$

$Y3c = 0.015$

and obtain:

$$\rho c = 0.00815 \text{ gmole/cc}$$

c) Reduced average density of diffusing mixture:

$\rho r = \bar{\rho}/\rho c$ and obtain:

$$\rho r = 0.9681$$

using Equation (46) obtain:

$$\frac{\rho_{ij} \mathcal{D}_{ij}}{\rho_{ij} \mathcal{D}_{ij}} = 0.91215$$

Critical properties of components 1, 2 and 3

component	critical pressure	critical temperature	critical molar volume	molecular weight
i	Pc (atm)	Tc (k°)	Vc (cc/gmole)	MW
1	45.78	190.5	99.392	16
2	37.46	425.0	225.24	58
3	21.69	618.0	596.12	142

Pseudo critical properties of binary system (i,j)

binary system	pseudo critical pressure	pseudo critical temperature	pseudo critical molar volume	pseudo critical compres-sibility
(i,j)	pPc (atm)	pTc (K°)	pVc (cc/gmole)	pZc
(1,2)	42.45	284.3	149.73	0.2725
(1,3)	33.10	415.5	360.83	0.3503
(2,3)	27.60	545.6	457.0	0.2818

Estimation of energy parameter, collision parameter and average molar density of components (i,j) in average diffusing mixture

binary system	energy parameter	collision diameter	average molar density
(i,j)	k/εij (k°)	σij (A)	ρij (gmole/cc)
(1,2)	0.00581	4.7081	0.00901
(1,3)	0.00161	4.6684	0.00742
(2,3)	0.00268	6.5574	0.00613

Estimation of collision integral Ωij

binary system	k/εij	T*=(k/εij)T	Ωij=Ω(1,1)*(T*)
(i,j)	(k°)		
(1,2)	0.00581	2.00	1.075
(1,3)	0.00161	0.55	1.966
(2,3)	0.00268	0.92	1.501

Estimation of mutual diffusion coefficients $\mathcal{D}_{ij}$

binary system (i,j)	$\rho_t \mathcal{D}_{ij}$ (EQ 47) (gmole/cc).cm²/sec	$\mathcal{D}_{ij}$ (EQ 46) (cm²/sec)
(1,2)	0.4977E-5	50.4E-5
(1,3)	0.2585E-5	31.8E-5
(2,3)	0.1014E-5	15.1E-5

Estimation of effective diffusion coefficients, Dim

component (i)	Dim (EQ 52) (cm²/sec)
1	36.9 E-5
2	22.6 E-5
3	22.0 E-5

Estimation of effective dispersion coefficient in porous media, Kim

component i	Kim=Dim/F (cm^2/sec)	K'im=Dim/FØ (cm^2/sec)
1	5.27 E-5	17.57 E-5
2	3.23 E-5	10.77 E-5
3	3.14 E-5	10.47 E-5

F: the formation resistivity factor is estimated from Archie's equation for sands, $F = 0.62/\emptyset^2 = 0.62/0.09 = 7.0$

2) Composition Profiles of Each Component i Using Equations (41) and (42).

The composition profiles are given by:

$$Yie = \bar{Yio} + \frac{1}{2}\,\mathrm{erfc}\left(\frac{XD}{2\sqrt{Kim\ t}}\right)(\dot{Yio} - \bar{Yio})_{i=1,3}$$

with the following normalization we obtain:

$$Yi = \frac{Yie}{\sum_{i=1}^{3} Yie}$$

The concentration distributions as a function of length traveled with respect to the initial interface is shown on Table 4.

TIME = 25.000 YEARS

CONCENTRATION DISTRIBUTION WRT LENGTH
SOLUTION OF THE EXACT SOLUTION APPROXIMATED BY THE ERFC FUNCTION

POSITION XD FROM INITIAL INTERFACE (CM)	MOLE FRACTION OF COMPONENT 1 METHANE	MOLE FRACTION OF COMPONENT 2 BUTANE	MOLE FRACTION OF COMPONENT 3 DECANE
-200.00	0.88947	0.08278	0.02774
-180.00	0.89051	0.08202	0.02747
-160.00	0.89156	0.08124	0.02720
-140.00	0.89261	0.08046	0.02692
-120.00	0.89367	0.07969	0.02665
-100.00	0.89472	0.07891	0.02637
-80.00	0.89577	0.07813	0.02610
-60.00	0.89682	0.07734	0.02583
-40.00	0.89789	0.07656	0.02555
-20.00	0.89894	0.07578	0.02528
-0.0	0.90000	0.07500	0.02500
20.00	0.90106	0.07422	0.02472
40.00	0.90211	0.07344	0.02445
60.00	0.90317	0.07266	0.02417
80.00	0.90423	0.07187	0.02390
100.00	0.90528	0.07109	0.02362
120.00	0.90634	0.07031	0.02335
140.00	0.90739	0.06953	0.02308
160.00	0.90845	0.06875	0.02280
180.00	0.90950	0.06797	0.02253
200.00	0.91055	0.06720	0.02226

Figure 32 represents the phase behaviour of the methane - n-butane - n-decane system at P=13783kpa and T=71c. Also, the composition paths of the two cases where, Case 1 corresponds to the situation where the species are diffusing with different diffusivities, and Case 2 is the case for a common diffusivity, are drawn. It may be noted that Case 1 corresponds to the case where molecular diffusion is the controlling process. On the other hand, Case 2 corresponds to the situation where convective mixing is the controlling process. If one examines equation (38):

$$Kim = \frac{Dim}{F} + \sigma \cdot Vd \cdot dp$$

a) for small darcy velocity Vd, Vd=0:

$\sigma Vd\ dp << Dim/F$ and $Kim = Dim/F$ (molecular diffusion controls)

b) for high darcy velocity Vd :

$\sigma Vd\ dp >> Dim/F$ and $Kim = \sigma Vd\ dp$ (convective mixing controls)

We may remark that in this case, Kim is the same for each component, that is components will diffuse with a common diffusivity.

At normal reservoir conditions, molecular diffusion is the controlling process. For the case studied, the effect of components diffusing with different diffusivities resulted in a composition path that did not cross the phase envelope. Hence, miscibility would not be expected to be lost due to this effect. Also the criterion defining first-contact

FIG 32

COMPARISON OF COMPOSITION PATH

ON THE PHASE DIAGRAM

CASE 1: COMPONENTS DIFFUSING WITH DIFFERENT EFFECTIVE DIFFUSIVITIES

CASE 2: COMPONENTS DIFFUSING WITH A COMMON EFFECTIVE DIFFUSIVITY

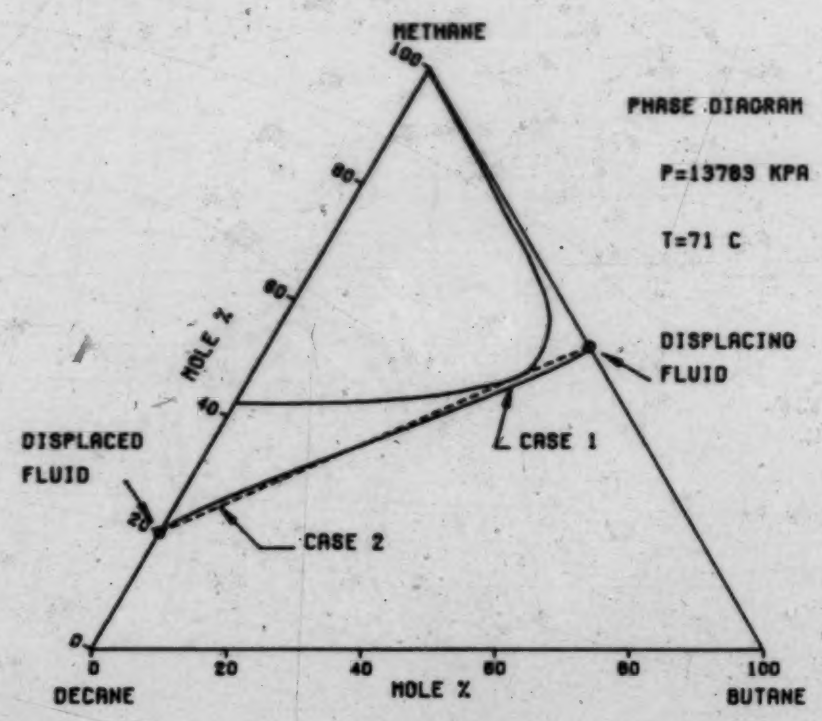

miscibility (line joining the points representing the compositions of the displacing and displaced fluids should not cross the phase envelope) is still applicable despite this effect. Let us consider the case where the displacing fluid composition is such, so that the line joining the point representing the composition of the displacing fluid to the point representing the composition of the displaced fluid barely crosses the phase envelope (see Case 2 of Figure 32). It may be concluded that this is the case of a multiple-contact miscible displacement. However, the effect of components diffusing with different diffusivities will tend to move the composition path away from the phase envelope. Hence, such a displacement should be more appropriately termed a first-contact miscible displacement.